Doctoral Dissertation

Formation mechanisms of mouse neural crest-derived stem cells

（マウス神経冠細胞由来幹細胞の形成機構）

Kyohei Fujita

Department of Biological Sciences

Graduate School of Science

Osaka University

2015

Table of contents

List of Figures

List of Tables

List of Abbreviations

°C	degrees Celsius
α-MEM	α-modified minimum essential medium
µChIP	micro chromatin immunoprecipitation
µg	microgram
µm	micrometer
µM	micromolar
BIO	6-Bromoindirubin-3'-oxime
BMP	bone morphogenetic protein
BrdU	5-bromo-2'-deoxyuridine
CEE	extract of day-11 chick embryos
CHD7	chromodomain helicase DNA-binding protein 7
CO_2	carbon dioxide
DAPI	4',6-diamidino-2-phenylindole
DN	dominant-negative
DNA	deoxyribonucleic acid
DRG	dorsal root ganglia
E	embryonic day
EDTA	ethylenediaminetetraacetic acid
EGTA	ethylene glycol tetraacetic acid
EMT	epithelial-mesenchymal transition
ES	embryonic stem

ESET	SET domain, bifurcated 1
FA	formaldehyde
FBS	fetal bovine serum
FGF	fibroblast growth factor
FoxD3	forkhead box D3
GFAP	glial fibrillary acidic protein
h	hours
H3K4me1	histone H3 monomethyl Lys 4
H3K9	histone H3 Lys 9
HCl	hydrogen chloride
His	histidine
IF	immunofluorescence
IgG	immunoglobulin G
IHC	immunohistochemistry
min	minutes
ml	milliliter
MLL1	mixed lineage leukemia 1
mm	millimeter
mM	millimolar
Msx1	msh homeobox 1
NaBu	sodium butyrate
NaCl	sodium chloride
NCSC	neural crest-derived stem cell
NF	neurofilament L
ng	nanogram

nM	nanomolar
NP	neural plate
NT	neural tube
O/N	overnight
Oct3/4	octamer-binding transcription factor 3/4
p75	low-affinity neurotrophin receptor p75
Pax3/7	paired box 3/7
PBS	phosphate buffered saline
PCR	polymerase chain reaction
PFA	paraformaldehyde
PIC	phenol–chloroform–isoamylalcohol (25:24:1)
PRC2	polycomb repressive complex 2
qPCR	quantitative polymerase chain reaction
RIPA	radio-immunoprecipitation assay
RNA	ribonucleic acid
s	seconds
SDS	sodium dodecyl sulfate
Setd1a	SET domain containing 1A
SEM	standard error of the mean
Setd7	SET domain containing (lysine methyltransferase) 7
siRNA	small interfering RNA
SMA	α smooth muscle cell actin
Sox	SRY-related HMG-box gene
Suv39h1	suppressor of variegation 3-9
TCF	T-cell factor

TE	Tris-EDTA
Tris	Tris(hydroxymethyl)aminomethane
TSS	transcriptional start sites
Twist1	twist basic helix-loop-helix transcription factor 1
WT	wild type
Zic1	zinc finger protein of the cerebellum 1

General Introduction

The neural crest is a transient embryonic structure unique to the vertebrates. Neural crest cells are multipotent and give rise to a diverse array of cell types, such as peripheral neurons and glia, smooth muscle cells, bones and cartilage of the head, melanocytes, and adipocytes [1, 2]. Neural crest cells are generated at the neural fold, the junction of the neural plate and the ectoderm, in response to BMPs/Wnts signaling [3-5]. These signals promote the expression of neural crest inducer genes including *Msx1*, *Pax3/7*, and *Zic1* [6]. Neural crest inducer genes activate the expression of neural crest specifier genes, such as *FoxD3*, *Sox9*, *Sox10*, *Slug*, and *Twist1* [7, 8]. Especially, Sox10 has been known to be an important factor for the maintenance of the undifferentiated state of neural crest cells [9]. After neural crest specification, neural crest cells undergo an EMT, delaminate from the dorsal aspect of the neural tube, and migrate throughout the embryo. Some neural crest cells maintain the multipotency and form NCSCs [10-13]. NCSCs are found in various adult tissues, such as DRG [14. 15], sciatic nerve [16, 17], and bone marrow [15]. NCSCs are typical tissue-specific stem cells with self-renewal capability and express p75 [16, 18, 19], a marker of undifferentiated neural crest cells [20]. However, little is known about the formation mechanisms of these cells.

Recently, CHD7 has been shown to play important roles in neural crest induction [21]. CHD7 is a member of ATP-dependent chromatin remodeling CHD family and characterized by the presence of two chromodomains, centrally located helicase domains [22]. In the neural crest induction, CHD7 activates the neural crest specifier genes, *Sox9*, *Twist1*, and *Slug* by binding to their enhancer elements marked with H3K4me1 [21]. CHD7 has been also shown to promote the migration of *Xenopus* neural crest cells [21].

Mutation of *CHD7* gene causes CHARGE syndrome, a multiple anomaly condition characterized by coloboma, heart defect, atresia choanae, retarded growth and development, genital abnormality, and ear abnormality [22-24]. This syndrome is due to abnormal development of the neural crest. In mouse ES cells, furthermore, CHD7 co-localizes with Oct3/4, Sox2, and Nanog at active gene enhancer elements showing high levels of H3K4me1/2 and act on the maintenance of the pluripotency of ES cells [25]. In the cardiomyocyte cells, CHD7 shows the direct binding to G/S and AR2 enhancers of *Nkx2.5* in a BMP-dependent manner [26]. In addition, CHD7 interacts with Sox2 and coordinately regulate the common target genes, such as *Jagged1* and *Mycn*, in neural stem cells [27]. CHD7 has been also known to be a critical regulator of the quiescence of neural stem cells in the adult hippocampus [28]. These findings show that CHD7 plays multiple roles in the regulation of transcriptional activities in various cell types.

In present studies, we analyzed the maintenance mechanisms of the multipotency of mouse trunk neural crest cells, leading to the formation of mouse NCSCs. CHD7 expression was observed in early migratory and undifferentiated mouse trunk neural crest cells expressing Sox10 and p75. The treatment with BMP2 and Wnt3a or the overexpression of CHD7 maintained the expression of CHD7, Sox10, and/or p75 in the undifferentiated neural crest cells. Furthermore, the inhibition of CHD7 expression significantly suppressed the maintenance of the undifferentiated state of these cells. These data suggest that this chromatin remodeler as well as BMP2/Wnt3a signaling play essential roles in the maintenance of the undifferentiated state of mouse trunk neural crest cells. In addition, clonal analysis of the neural crest cells showed that BMP2/Wnt3a signaling and CHD7 promote the maintenance of the multipotency of these cells. Thus, it is possible that BMP2/Wnt3a signaling and CHD7 maintain the multipotency of mouse trunk neural crest cells and lead to the formation of mouse NCSCs. Furthermore, we analyzed a

regulatory gene cascade in the formation of mouse NCSCs. The inhibition of FoxD3 expression significantly suppressed the expression of Sox10, which is an indispensable transcription factor for mouse NCSC formation, in the presence of BMP2/Wnt3a. CHD7, Oct3/4, Sox2, and Nanog bound to the *cis*-regulatory regions of mouse *FoxD3* (mE1, mE2, and mE3) in a BMP2/Wnt3a-dependent manner. In addition, these *cis*-elements contained the binding sites of CHD7, Oct3/4, Sox2, and Nanog. Furthermore, siRNAs of *CHD7*, *Oct3/4*, *Sox2*, and *Nanog* significantly suppressed the expression of FoxD3 and Sox10. The inhibition of histone H3K4 mono- or tri-methylation also repressed FoxD3 expression. The present data suggest that CHD7, Oct3/4, Sox2, and Nanog directly induce FoxD3 expression when stimulated by BMP2/Wnt3a signaling, that FoxD3 promotes Sox10 expression, and that histone H3K4 methylation plays important roles in this process of mouse NCSC formation. Thus, the formation mechanism of mouse NCSCs is dramatically different from the induction mechanisms of neural crest cells.

Chapter I

Roles of chromatin remodeler in maintenance mechanisms of multipotency of mouse trunk neural crest cells in the formation of neural crest-derived stem cells

Introduction

The neural crest is a transient embryonic structure in vertebrates. Neural crest cells arise within the neural fold, migrate ventrally and laterally (Fig. 1.1A), and contribute to a wide variety of cell types, such as peripheral neurons and their supportive cells, pigment cells, skeletal derivatives, adipocytes, endocrine cells, and smooth muscle cells [1, 2] (Fig. 1.1B). Recent studies have revealed that some neural crest cells maintain multipotency and form NCSCs [10-13]. NCSCs have been shown to exist in late embryonic and adult tissues such as DRG [14, 15], sciatic nerve [16, 17], gut [18, 19], heart [29], hair follicle [30], and bone marrow [15] (Fig. 1.2). However, little is known about the formation mechanisms of NCSCs.

It has been shown that BMP and Wnt are involved not only in neural crest induction in chick and *Xenopus* [3-5] but also in the maintenance of the undifferentiated state of neural crest cells in mouse and rat [31]. Moreover, a recent study has elucidated that CHD7, one of chromatin remodelers, plays important roles in neural crest induction by controlling the expression of neural crest specifier genes [21]. CHD7 also interacts with three master regulators of multipotency, Oct3/4, Sox2, and Nanog, in ES cells [25]. The mutation of this remodeler gene causes the CHARGE syndrome by abnormal neural crest development

[22-24]. These findings suggest that CHD7 as well as BMP/Wnt signaling may be involved in maintaining of the multipotency of neural crest cells and conduct them to mouse NCSCs. In the present study, therefore, we analyzed roles of CHD7 and BMP/Wnt signaling in maintaining the multipotency of mouse trunk neural crest cells, leading to the formation of mouse NCSCs.

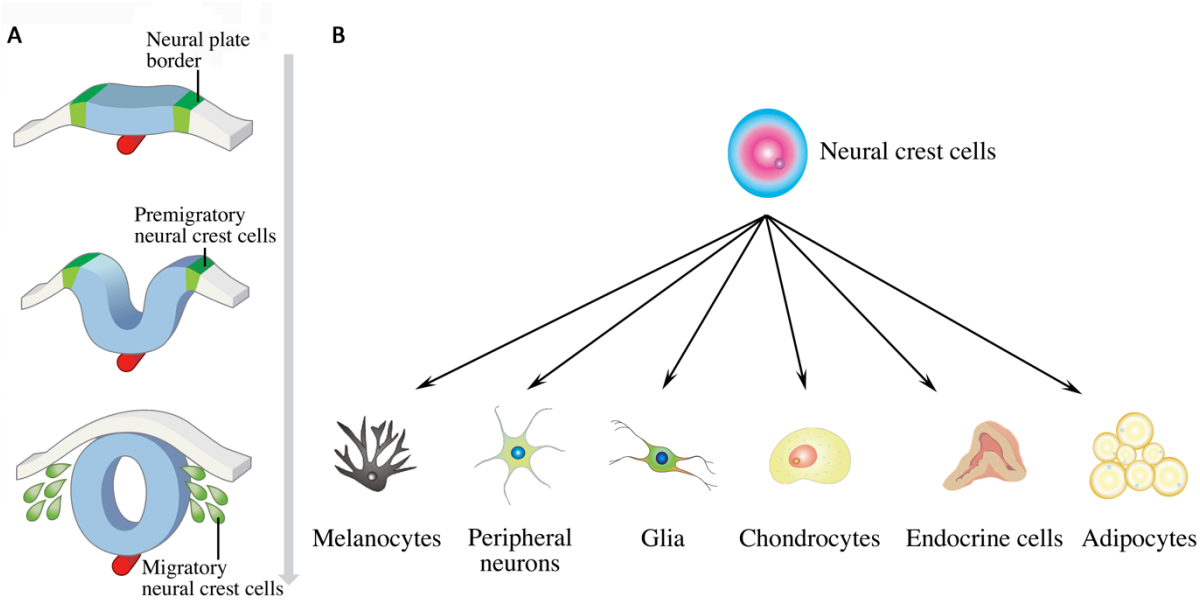

Fig. 1.1 Development of the neural crest. **(A)** The neural crest is induced at the neural plate border (green), the boundary of the neural ectoderm (blue) and the epidermis (white). After EMT, neural crest cells delaminate from dorsal aspects of the neural tube and migrate throughout the embryo. **(B)** Neural crest cells differentiate into diverse cell types, such as melanocytes, peripheral neurons and glia, chondrocytes, endocrine cells, and adipocytes. Figure 1.1A redrawn after Green et al. (2015) [32].

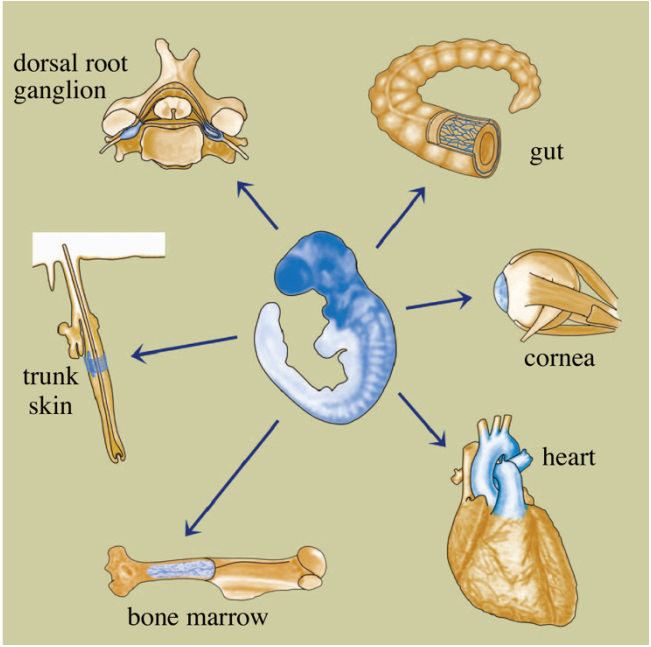

Fig. 1.2 Distribution of NCSCs. NCSCs are present in various adult tissues including dorsal root ganglion, gut, cornea, heart, bone marrow, and skin. Figure redrawn after Shakhova and Sommer (2010) [11].

Materials & Methods

Primary and clonal cultures

Primary cultures of mouse trunk neural crest cells were prepared from ddY mouse embryos at E9.5 (24- to 29-somite stages) [33-35]. Neural tubes were isolated from the dorsal trunk region at the last six-somite levels of E9.5 embryos. Neural tubes were explanted into 35-mm culture dishes coated with collagen gel (PureCol). The explants were scraped away with a tungsten needle after 48 h in culture, leaving the emigrated trunk neural crest cells on the substratum.

Clonal cultures of the trunk neural crest cells were performed by a modification of methods described previously [33, 36]. Neural crest cells were resuspended by trypsinization after 6 days in culture. This essentially single cell suspension (> 90% single cells) was diluted with culture medium, and 1 ml aliquots of this cell suspension were seeded at 500 cells/ml onto 35-mm culture dishes coated with a collagen gel and conditioned with culture medium containing 10 μg/ml plasma fibronectin (Itoham). The clone founder cells were identified at 8 h after seeding cells. The efficiency of clone formation was 5.5 (± 1.5)%.

The culture medium consisted of 85% α-MEM (Sigma), 10% FBS (GE Healthcare Life Sciences), 5% CEE, and 50 μg/ml gentamicin (Sigma). The cultures were incubated at 37°C in a humidified atmosphere containing 5% CO_2. The culture medium was changed every other day. BMP2 (R&D Systems), Wnt1 (PEPROTECH), and Wnt3a (R&D Systems) were added to the medium at a concentration of 10 or 100 ng/ml. FGF2 (R&D Systems) was added to the medium at a concentration of 10 ng/ml. Chordin (R&D

Systems), Noggin (R&D Systems), and BIO (Calbiochem) were added at concentrations of 1 μg/ml, 100 ng/ml, and 1 μM, respectively.

Transfection of expression vectors

Mouse trunk neural crest cells were transfected with 1 μg of expression vectors for 24 h immediately after the removal of the neural tubes, using Lipofectamine 2000 (Invitrogen). Expression vectors are listed in Table 1.1. pcDNA3.1 (Invitrogen) was used as the control vector. The transfection efficiency of the vectors encoding a myc epitope or a Flag tag was estimated by immunostaining using mouse anti-c-myc or mouse anti-Flag. The transfection efficiency was presented as the proportion of cells expressing the myc epitope or the Flag tag per total cells in a neural crest cell colony. The percentage of cells expressing the myc epitope or the Flag tag reached 52.7 (± 3.5) or 72.2 (± 2.8)%.

Table 1.1 List of expression vectors

Expression Vectors	
pcDNA3 encoding the human DN TCF and a myc-tag	A gift from Dr. Jane B. Trepel [37, 38]
pcDNA4 encoding the mouse DN β-catenin and a His-tag	A gift from Dr. Jane B. Trepel [37, 38]
pcDNA3.1 encoding the human WT CHD7 and a Flag-6×His-tag	A gift from Dr. J. Wysocka [21]
pcDNA3.1 encoding the human DN CHD7 and a Flag-6×His-tag	A gift from Dr. J. Wysocka [21]

***CHD7* siRNA preparation**

CHD7 siRNA was prepared as described previously [39, 40]. The siRNA duplex for *CHD7* were designed on the basis of *CHD7* sequence published online [GenBank Accession

No. NM001081417]. The sequence corresponded to bases 4481-4506 of the open reading frame of *CHD7* mRNA: 5'-CAGGCTCAAGCTAGATGCCACAGAA (prepared by Invitrogen). Stealth™ RNAi Negative Control Medium GC Duplex #2 (Invitrogen) was used as the control for *CHD7* siRNA. Using Lipofectamine 2000, mouse trunk neural crest cells were transfected with 40 nM *CHD7* siRNA or RNAi Negative Control for 24 h immediately after the removal of the neural tubes. The transfection efficiency was examined by means of BLOCK-iT Fluorescent Oligo (Invitrogen). The percentage of cells showing a fluorescent signal per neural crest cell colony reached 98.4 ± 0.49%.

Immunostaining

Primary cultures of mouse trunk neural crest cells were fixed with 4% PFA for 1 h on ice. The cultures were immunostained with the primary antibodies for 16 h at 4°C and with the secondary antibodies for 1 h at room temperature.

E9.5 mouse embryos, DRG dissected from 11- to 12-week-old ddY mice, and sciatic nerve from L3 to L5 in 11- to 12-week-old ddY mice were fixed with 4% PFA for 1 or 2 h on ice. The fixed tissues were immersed in gradually increasing concentrations of sucrose solution and embedded in OCT compound (Miles). Cryostat sections were cut at 10 μm and mounted on albumin-coated glass slides. The sections were stained using the primary antibodies. Primary antibodies were applied for 16 h at 4°C. The specimens were treated with the secondary antibodies at room temperature for 1 h. Finally, the cultures and sections were nuclear-stained with 0.1 μg/ml DAPI (Dojindo). DAPI nuclear staining was particularly important for counting the exact number of immunoreactive cells in the neural crest cell cultures and for judging cell death. All antibodies are listed in Table 1.2.

Table 1.2 Antibodies used for immunostaining

Antigen/Conjugation	Dilution	Catalog number
Sox10 (rabbit polyclonal antibody)	1:100 (IF) 1:200 (IHC)	MILLIPORE (AB5727)
CHD7 (goat polyclonal antibody)	1:100 (IF) 1:50 (IHC)	Santa Cruz (sc-79207)
p75 (rabbit polyclonal antibody)	1:100 (IF) 1:100 (IHC)	Promega (G323A)
NF (rabbit polyclonal antibody)	1:500	MILLIPORE (AB9568)
SMA (1A4, mouse monoclonal IgG2a)	1:800	Sigma (A2547)
GFAP (rabbit polyclonal antibody)	1:100	Dako (Z0334)
BrdU (B44, mouse monoclonal IgG1)	1:10	Becton Dickinson (347580)
Caspase-3 p11 (mouse monoclonal IgG1)	1:50	Santa Cruz (sc-271759)
Alexa Fluor 488 (Donkey anti-Goat IgG)	1:500	Invitrogen (A-11055)
Alexa Fluor 488 (Donkey anti-Mouse IgG)	1:500	Invitrogen (A-21202)
Alexa Fluor 555 (Donkey anti-Rabbit IgG)	1:500	Invitrogen (A-31572)

Measurement of cell proliferation and apoptosis

BrdU-labeling experiments were performed to estimate cell proliferation in mouse trunk neural crest cell cultures. BrdU (Wako) was prepared as a 1 mM stock solution in α-MEM and added to the cultures at a final concentration of 50 μM. The cultures were exposed to BrdU for 90 min and subsequently fixed in 4% PFA on ice for 1 h. BrdU-incorporated cells were detected with anti-BrdU. Furthermore, we characterized the developmental cell death of the trunk neural crest cells by measuring the expression of the apoptotic marker, caspase-3. The cultures were fixed in 4% PFA on ice for 1 h and double-stained with anti-Sox10 and anti-caspase-3 or with anti-p75 and anti-caspase-3. The cultures were nuclear-stained with 0.1 μg/ml DAPI for the total cell count.

Results

CHD7 expression in trunk neural crest cells of mouse embryos

Since there have been no reports of CHD7 expression in mouse neural crest cells, we examined the expression patterns of CHD7 in trunk neural crest cells of mouse embryos. We performed the double-stainings using anti-CHD7 and antibodies against Sox10, which is known to be involved in the maintenance of the undifferentiated state of neural crest cells [9], or against p75, another marker of undifferentiated neural crest cells [20]. No expression of CHD7, Sox10, and p75 were observed at the unsegmented levels of the 28-somite stage embryos (Fig. 1.3A-J). At 26-somite levels of the 26-somite stage embryos, CHD7 expression was found in early migratory neural crest cells containing Sox10 or p75 (arrows in Fig. 1.3L-O and Q-T). Furthermore, cells that express both CHD7 and Sox10 were observed in the dorsal neural tube containing premigratory neural crest cells (arrowheads in Fig. 1.3L-O). In addition, there existed CHD7-expressing cells with both Sox10 and p75 at the 25-somite levels of the 28-somite stage embryos (data not shown). We also examined the expression of CHD7, Sox10, and p75 during late migratory stages of the trunk neural crest cells. CHD7-expressing cells containing Sox10 and/or p75 were observed (arrows in Fig. 1.3V-Y and A'-D'). These results indicate that undifferentiated mouse trunk neural crest cells express CHD7 as well as Sox10 and p75.

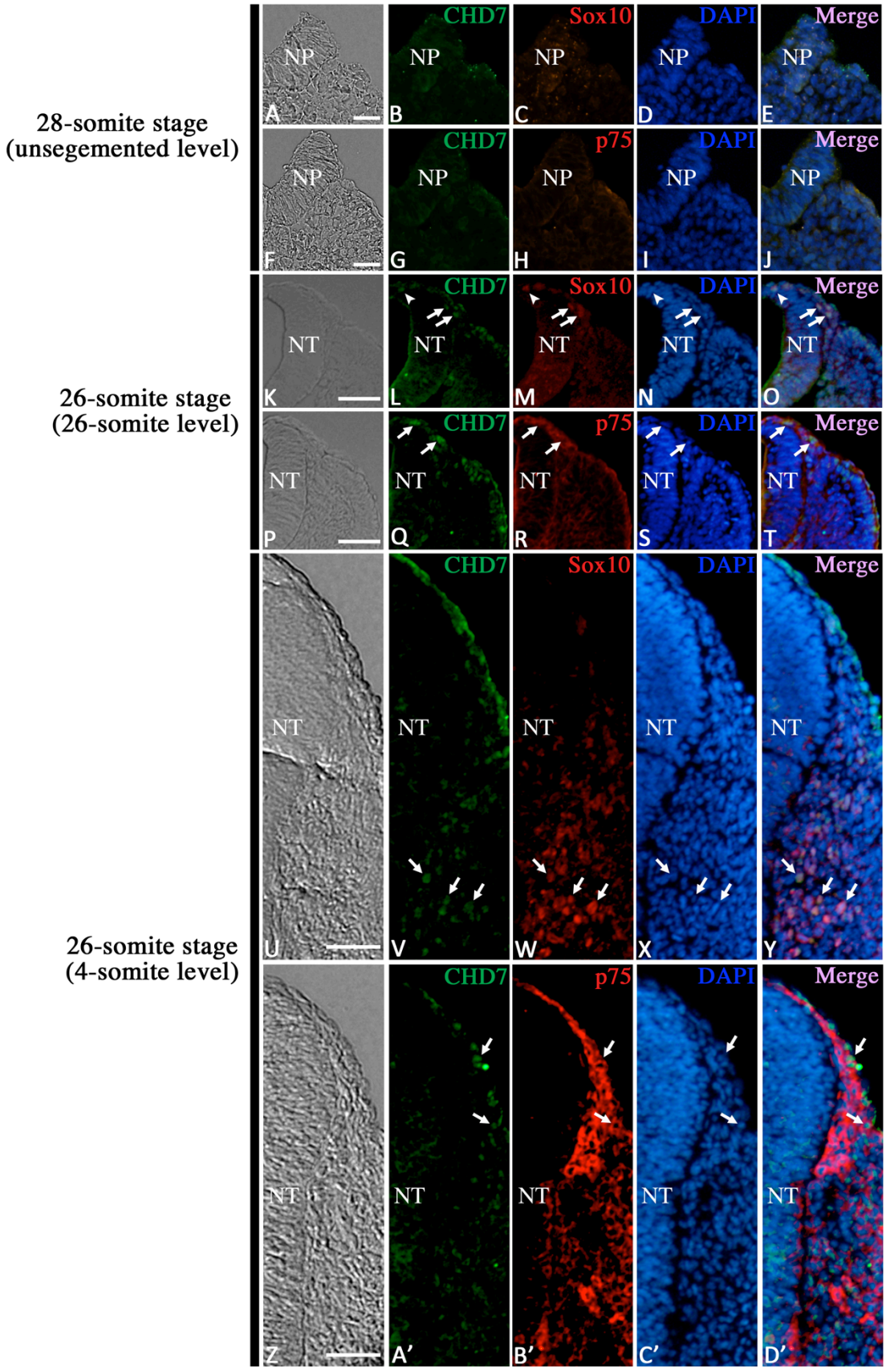
28-somite stage
(unsegemented level)
26-somite stage
(26-somite level)
26-somite stage
(4-somite level)
NP
NT
CHD7
Sox10
p75
DAPI
Merge
A
B
C
D
E
F
G
H
I
J
K
L
M
N
O
P
Q
R
S
T
U
V
W
X
Y
Z
A'
B'
C'
D'

Fig. 1.3 Expression patterns of CHD7, Sox10, or p75 during mouse trunk neural crest development. The top, bottom, left, and right of each photograph correspond to the dorsal, ventral, proximal, and distal side of the embryo, respectively. **(A-J)** Transverse sections of a 28-somite stage embryo at the unsegmented level. (A-E) and (F-J) are neighboring sections. **(A)** Bright-field image. **(B)** Expression pattern of CHD7 in the same field as (A). **(C)** Expression pattern of Sox10 in the same field as (A). **(D)** DAPI nuclear stain of the same field as (A). **(E)** Merged image of (B-D). **(F)** Bright-field image. **(G)** Expression pattern of CHD7 in the same field as (F). **(H)** Expression pattern of p75 in the same field as (F). **(I)** DAPI nuclear stain of the same field as (F). **(J)** Merged image of (G-I). **(K-T)** Transverse sections of a 26-somite stage embryo at the 26-somite level. (K-O) and (P-T) are neighboring sections. **(K)** Bright-field image. **(L)** Expression pattern of CHD7 in the same field as (K). **(M)** Expression pattern of Sox10 in the same field as (K). **(N)** DAPI nuclear stain of the same field as (K). **(O)** Merged image of (L-N). **(P)** Bright-field image. **(Q)** Expression pattern of CHD7 in the same field as (P). **(R)** Expression pattern of p75 in the same field as (P). **(S)** DAPI nuclear stain of the same field as (P). **(T)** Merged image of (Q-S). **(U-D')** Oblique sections of a 26-somite stage embryo at the 4-somite level. (U-Y) and (Z-D') are neighboring sections. **(U)** Bright-field image. **(V)** Expression pattern of CHD7 in the same field as (U). **(W)** Expression pattern of Sox10 in the same field as (U). **(X)** DAPI nuclear stain of the same field as (U). **(Y)** Merged image of (V-X). **(Z)** Bright-field image. **(A')** Expression pattern of CHD7 in the same field as (Z). **(B')** Expression pattern of p75 in the same field as (Z). **(C')** DAPI nuclear stain of the same field as (Z). **(D')** Merged image of (A'-C'). Arrows indicate the neural crest cells expressing both CHD7 and Sox10 or both CHD7 and p75. Arrowheads show a cell expressing both CHD7 and Sox10 in the dorsal neural tube that the premigratory neural crest cells exist. NP; neural plate, NT; neural tube. Scale Bars = 20 μm.

Expression of CHD7, Sox10, and p75 in mouse trunk neural crest cell cultures

Mouse trunk neural crest cells undergo temporally regulated differentiation even in cultures [33, 34]. Therefore, to examine the temporal changes in CHD7 expression, we used mouse trunk neural crest cell cultures. After 2, 4, or 6 days in culture, we performed immunocytochemical analysis using anti-CHD7 and anti-Sox10. The percentage of cells expressing CHD7 and/or Sox10 per neural crest cell colony (each colony of neural crest cells was derived from a neural tube explant) was significantly lower at 6 days in culture than at 2 days in culture (Fig. 1.4A-M). Experiments using anti-CHD7 and anti-p75 also showed the same results (Fig. 1.4N-Z).

Actions of BMP and Wnt signaling on the maintenance of the undifferentiated state of mouse trunk neural crest cells

It has been known that the concerted activity of BMP2 (10 ng/ml) and Wnt1 (unknown concentrations) maintains the undifferentiated state of neural crest cells [18]. Therefore, we examined whether these factors not only participate in the maintenance of the undifferentiated state of mouse trunk neural crest cells under our experimental conditions but also affect CHD7 expression in these cells. BMP2 and Wnt1 were added to the medium from 2 days to 6 days in culture (Fig. 1.5A). When Wnt1 was used at 10 ng/ml, the expression of CHD7 and/or p75 was significantly maintained on culture day 6 (Fig. 1.5G and O-Q). The maintenance of Sox10 expression was less pronounced (Fig. 1.5H). However, in the treatment with 100 ng/ml Wnt1 and 10 ng/ml BMP2, Sox10 expression drastically decreased (Fig. 1.5H). Furthermore, the percentage of double-positive cells expressing Sox10 and CHD7 was also suppressed (Fig. 1.5I). Therefore, we used Wnt3a, which is

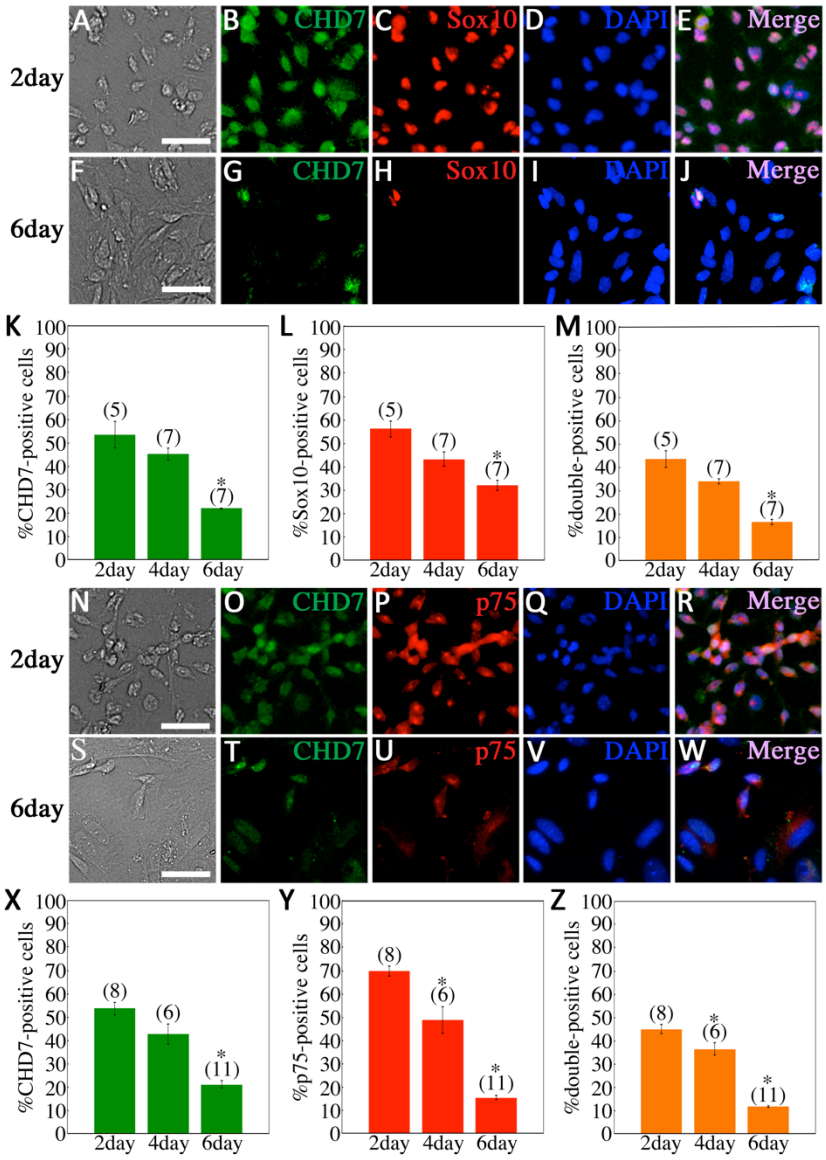

Fig. 1.4 Expression patterns of CHD7, Sox10, or p75 in mouse trunk neural crest cell cultures. Immunostaining with anti-CHD7, anti-Sox10, and anti-p75 was performed on culture day 2, 4, and 6. **(A and F)** Bright-field images. **(B and G)** Anti-CHD7-positive cells in the same fields as (A) and (F), respectively. **(C and H)** Anti-Sox10-positive cells in the same fields as (A) and (F), respectively. **(D and I)** DAPI nuclear stains of the same fields as (A) and (F), respectively. **(E)** Merged image of (B-D). **(J)** Merged image of (G-I). **(K)** Percentage of cells expressing CHD7 per total cells in a neural crest cell colony (each colony was derived from a neural tube explant). **(L)** Percentage of cells expressing Sox10 per total cells in a neural crest cell colony. **(M)** Percentage of cells expressing both CHD7 and Sox10 per total cells in a neural crest cell colony. **(N and S)**

Bright-field images. **(O and T)** Anti-CHD7-positive cells in the same fields as (N) and (S), respectively. **(P and U)** Anti-p75-positive cells in the same fields as (N) and (S), respectively. **(Q and V)** DAPI nuclear stains of the same fields as (N) and (S), respectively. **(R)** Merged image of (O-Q). **(W)** Merged image of (T-V). **(X)** Percentage of cells expressing CHD7 per total cells in a neural crest cell colony. **(Y)** Percentage of cells expressing p75 per total cells in a neural crest cell colony. **(Z)** Percentage of cells expressing both CHD7 and p75 per total cells in a neural crest cell colony. *, $p < 0.05$ (Student's *t*-test) compared to culture day 2. Data in (K-M and X-Z) are expressed as mean ± SEM of separate counts of 5-11 colonies (the number in a parenthesis on each bar). Scale Bars = 50 μm.

---

expressed in the dorsal neural tube in which neural crest cells are formed, similar to Wnt1 [41]. The treatment with 10 ng/ml BMP2 and 10 ng/ml Wnt3a promoted the expression of CHD7, Sox10, or p75. The effects were unchanged even when Wnt3a was used at 100 ng/ml (Fig. 1.5). These results suggest that Wnt3a is more effective for the maintenance of the undifferentiated state of mouse trunk neural crest cells. Therefore, we examined the effects of BMP2, Wnt1, and Wnt3a in more detail. BMP2 or Wnt1 alone had almost no effects on CHD7 expression or inhibitory effects on Sox10 expression (Fig. 1.6B-D). These inhibitory effects may cause the decrease of Sox10 expression in BMP2/Wnt1 treatment, leading to the reduction of the proportion of cells expressing both Sox10 and CHD7. On the other hand, the treatment with Wnt3a alone, especially with 100 ng/ml Wnt3a, produced effects similar to those of the 10 ng/ml BMP2 and 10 ng/ml Wnt3a treatments on the maintenance of the undifferentiated state (Fig. 1.6B-D). We prevented BMP activities with two BMP inhibitors, noggin and chordin, to exclude the possibility that the effects of Wnt3a alone were caused by the BMP activities in FBS and/or CEE in the culture medium [42].

These inhibitors had no effects on the maintenance of CHD7 or Sox10 expression (Fig. 1.6E-G). These data suggest that the Wnt signaling is indispensable for the maintenance of the undifferentiated state of mouse trunk neural crest cells and BMP signaling plays supportive roles in the maintenance of the undifferentiated state of these cells.

We tried to identify the Wnt signaling pathway involved in the maintenance of the undifferentiated state. When the neural crest cell cultures were treated with 10 ng/ml BMP2 and BIO, a reagent that activates the Wnt/β-catenin pathway [43], effects similar to those of the 10 ng/ml BMP2 and 10 ng/ml Wnt3a treatments were produced (Fig. 1.6H-J). In addition, the treatment with the DN β-catenin expression vectors or the DN TCF expression vectors drastically inhibited the effects of 10 ng/ml BMP2 and 10 ng/ml Wnt3a on CHD7 or Sox10 expression (Fig. 1.6H-J). Thus, Wnt/β-catenin pathway may play important roles in the maintenance of the undifferentiated state of mouse trunk neural crest cells.

Previous studies have shown that the treatment with 10 ng/ml BMP2 [44] or unknown concentrations of Wnt1 [45, 46] promotes sensory neurogenesis of neural crest cells. Therefore, we investigated the effects of BMP2, Wnt1 and/or Wnt3a on sensory neurogenesis of mouse trunk neural crest cells under the present culture condition. The treatment with 10 ng/ml BMP2, Wnt1 (10 ng/ml or 100 ng/ml), and/or Wnt3a (10 ng/ml or 100 ng/ml) promoted the differentiation of sensory neurons containing Brn3a (Fig. 1.7), similar to previous reports. However, no synergistic effects of the treatment with both 10 ng/ml BMP2 and 10 ng/ml Wnt3a were found. These data suggest that the coordinated activity of BMP2 and Wnt3a acts on the maintenance of the undifferentiated state of mouse trunk neural crest cells rather than promotes differentiation of these cells into sensory neurons.

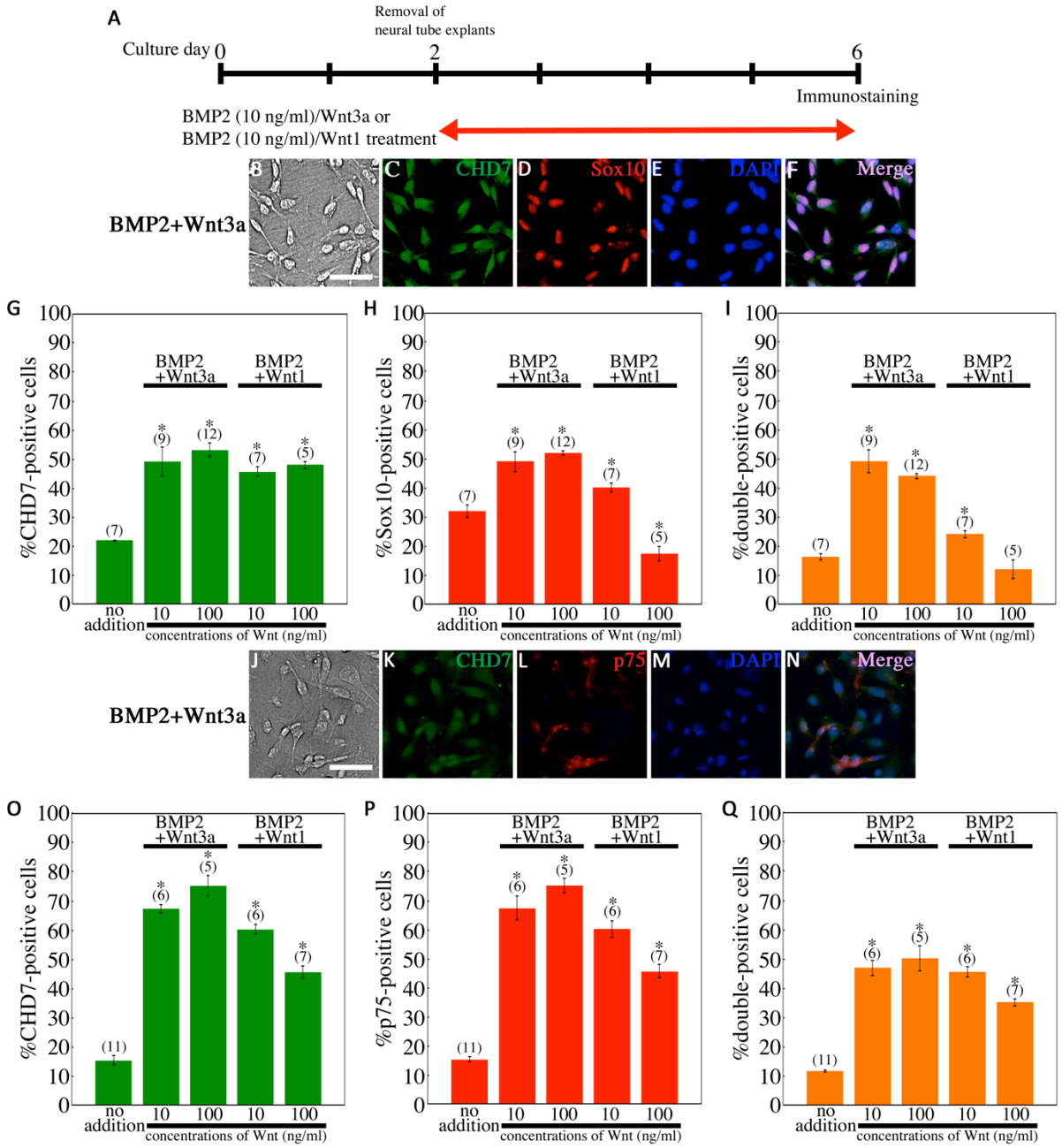

Fig. 1.5 Effects of BMP and Wnt on the maintenance of the undifferentiated state. **(A)** After removal of neural tube explants, mouse trunk neural crest cells were exposed to BMP2/Wnt3a or BMP2/Wnt1 from 2 days to 6 days in culture. Immunostaining with anti-CHD7 and anti-Sox10 or with anti-CHD7 and anti-p75 was performed on culture day 6. **(B)** Bright-field image in the presence of BMP2 and Wnt3a. **(C)** Anti-CHD7-positive cells in the same field as (B). **(D)** Anti-Sox10-positive cells in the same field as (B). **(E)** DAPI nuclear stain of the same field as (B). **(F)** Merged image of (C-E). **(G)** Percentage of cells expressing CHD7 per total cells in a neural crest cell colony (each

colony was derived from a neural tube explant). **(H)** Percentage of cells expressing Sox10 per total cells in a neural crest cell colony. **(I)** Percentage of cells expressing both CHD7 and Sox10 per total cells in a neural crest cell colony. **(J)** Bright-field image in the presence of BMP2 and Wnt3a. **(K)** Anti-CHD7-positive cells in the same field as (J). **(L)** Anti-p75-positive cells in the same field as (J). **(M)** DAPI nuclear stain of the same field as (J). **(N)** Merged image of (K-M). **(O)** Percentage of cells expressing CHD7 per total cells in a neural crest cell colony. **(P)** Percentage of cells expressing p75 per total cells in a neural crest cell colony. **(Q)** Percentage of cells expressing both CHD7 and p75 per total cells in a neural crest cell colony. *, $p < 0.05$ (Student's *t*-test) compared to the untreated cultures. Data in (G-I and O-Q) are expressed as mean ± SEM of separate counts of 5-12 colonies (the number in a parenthesis on each bar). Scale Bars = 50 μm.

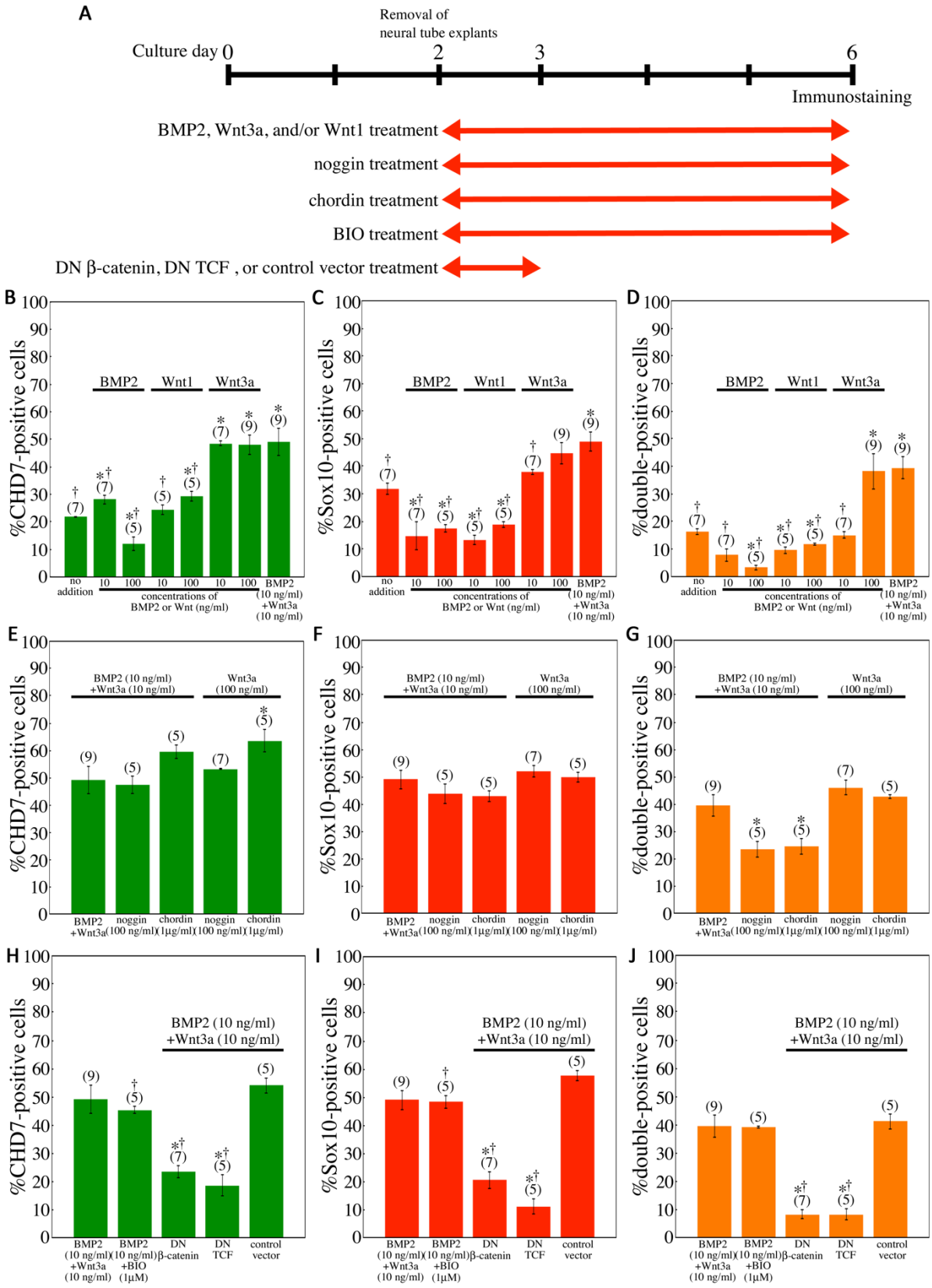

Fig. 1.6 Roles of Wnt/β-catenin pathway in the maintenance of the undifferentiated state.

(A) After removal of neural tube explants, mouse trunk neural crest cells were exposed to BMP2, Wnt1,

Wnt3a, noggin, chordin and/or BIO from 2 days to 6 days in culture. The DN β-catenin expression vectors, the DN TCF expression vectors, or the control vectors were applied from 2 days to 3 days in culture. Immunostaining with anti-CHD7 and anti-Sox10 was performed on culture day 6. **(B)** Percentage of cells expressing CHD7 per total cells in a neural crest cell colony (each colony was derived from a neural tube explant). **(C)** Percentage of cells expressing Sox10 per total cells in a neural crest cell colony. **(D)** Percentage of cells expressing both CHD7 and Sox10 per total cells in a neural crest cell colony. *, $p < 0.05$ (Student's *t*-test) compared to the untreated cultures. †, $p < 0.05$ (Student's *t*-test) compared to the BMP2/Wnt3a-treated cultures. **(E)** Percentage of cells expressing CHD7 per total cells in a neural crest cell colony. **(F)** Percentage of cells expressing Sox10 per total cells in a neural crest cell colony. **(G)** Percentage of cells expressing both CHD7 and Sox10 per total cells in a neural crest cell colony. **(H)** Percentage of cells expressing CHD7 per total cells in a neural crest cell colony. **(I)** Percentage of cells expressing Sox10 per total cells in a neural crest cell colony. **(J)** Percentage of cells expressing both CHD7 and Sox10 per total cells in a neural crest cell colony. *, $p < 0.05$ (Student's *t*-test) compared to the BMP2/Wnt3a-treated cultures. †, $p < 0.05$ (Student's *t*-test) compared to the cultures treated with the control vectors. Data are expressed as mean ± SEM of separate counts of 5-9 colonies (the number in a parenthesis on each bar).

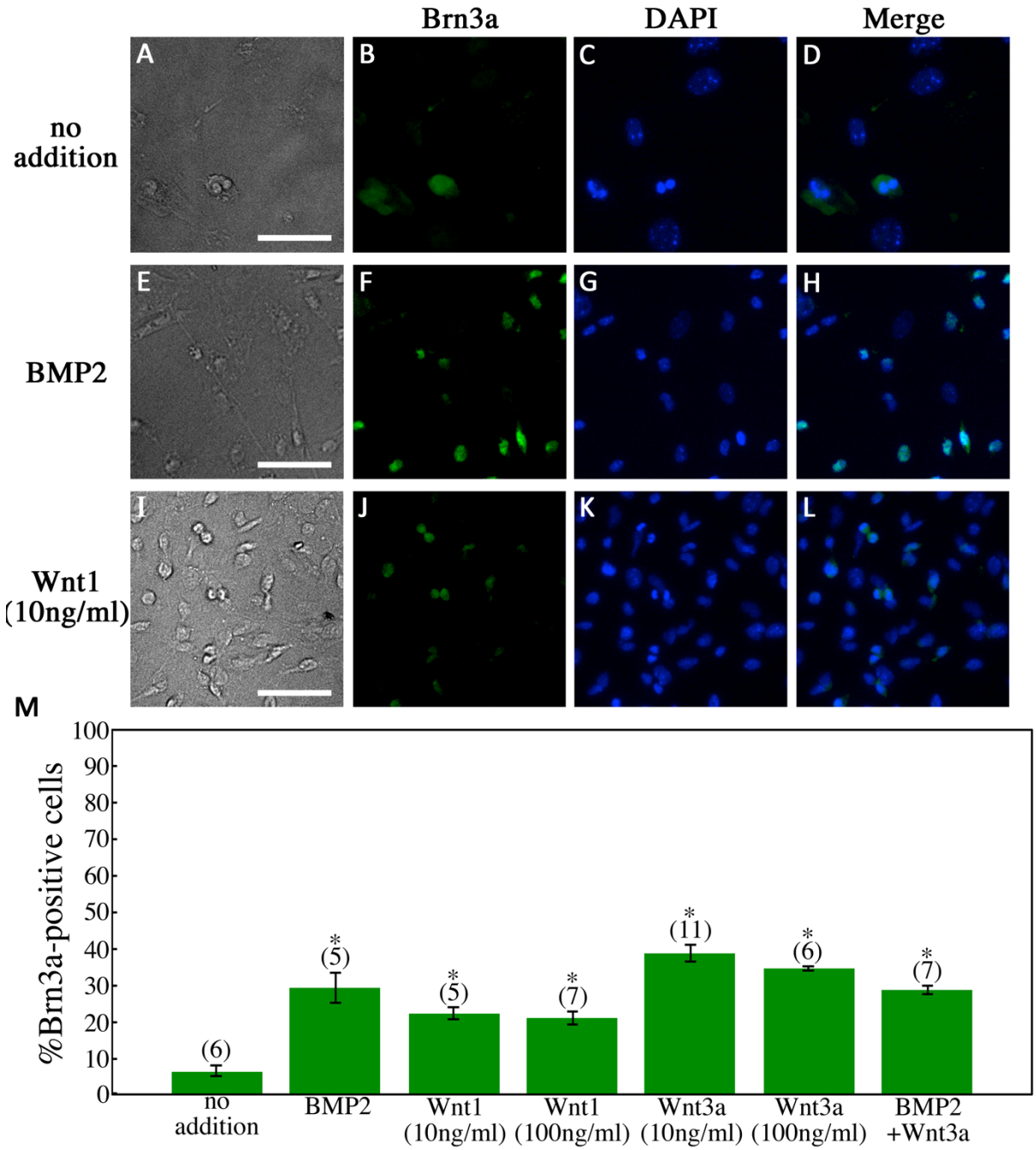

Fig. 1.7 Sensory neurogenesis in mouse trunk neural crest cell cultures. Immunostaining with anti-Brn3a was performed on culture day 6. **((A), (E), and (I))** Bright-field images. **((B), (F), and (J))** Anti-Brn3a-positive cells in the same fields as (A), (E), and (I), respectively. **((C), (G), and (K))** DAPI nuclear stains of the same fields as (A), (E), and (I), respectively. **(D)** Merged image of (B) and (C). **(H)** Merged image of (F) and (G). **(L)** Merged image of (J) and (K). **(M)** Percentage of cells expressing Brn3a per total cells in a neural crest cell colony (each colony was derived from a neural tube explant). *, $p < 0.05$ (Student's *t*-test) compared to the untreated cultures. Data are expressed

as mean ± SEM of separate counts of 5-11 colonies (the number in a parenthesis on each bar). Scale Bars = 50 μm.

Actions of CHD7 on the maintenance of the undifferentiated state of mouse trunk neural crest cells

In this study, we showed that BMP/Wnt signaling not only maintained the undifferentiated state of mouse trunk neural crest cells but also activated CHD7 expression. It is possible that CHD7 plays important roles in the maintenance of the undifferentiated state of mouse trunk neural crest cells. To examine this possibility, the neural crest cell cultures were treated with the WT CHD7, DN CHD7 expression vectors, or *CHD7* siRNA (Fig. 1.8A and Fig. 1.9A). The number of CHD7-positive cells was dramatically increased by the addition of the WT CHD7 expression vectors (Fig. 1.8C, G, K, and O). This showed that the WT CHD7 expression vectors were effectively introduced to the neural crest cells. Furthermore, the WT CHD7 expression vectors maintained the expression of Sox10 or p75 (Fig. 1.8D, H, L, and P) and the co-expression of CHD7 and Sox10 (Fig. 1.8F and I) or of CHD7 and p75 (Fig. 1.8N and Q). When the DN CHD7 expression vectors were added, the number of CHD7-positive cells increased (Fig. 1.9B and E), indicating that the anti-CHD7 antibody used in this study recognizes the mutant CHD7, because this mutant protein changed only lysine 998 in the ATPase domain of CHD7 to arginine. However, treatment with the DN CHD7 expression vectors significantly suppressed the expression of Sox10 and p75 (Fig. 1.9C and F). This treatment also suppressed the co-expression of CHD7 and Sox10 or of CHD7 and p75 (Fig. 1.9D and G). Treatment with *CHD7* siRNA dramatically suppressed the expression of CHD7, Sox10, and/or p75 (Fig. 1.9B-G). These results show

that CHD7 is a key requisite for the maintenance of the undifferentiated state of mouse trunk neural crest cells.

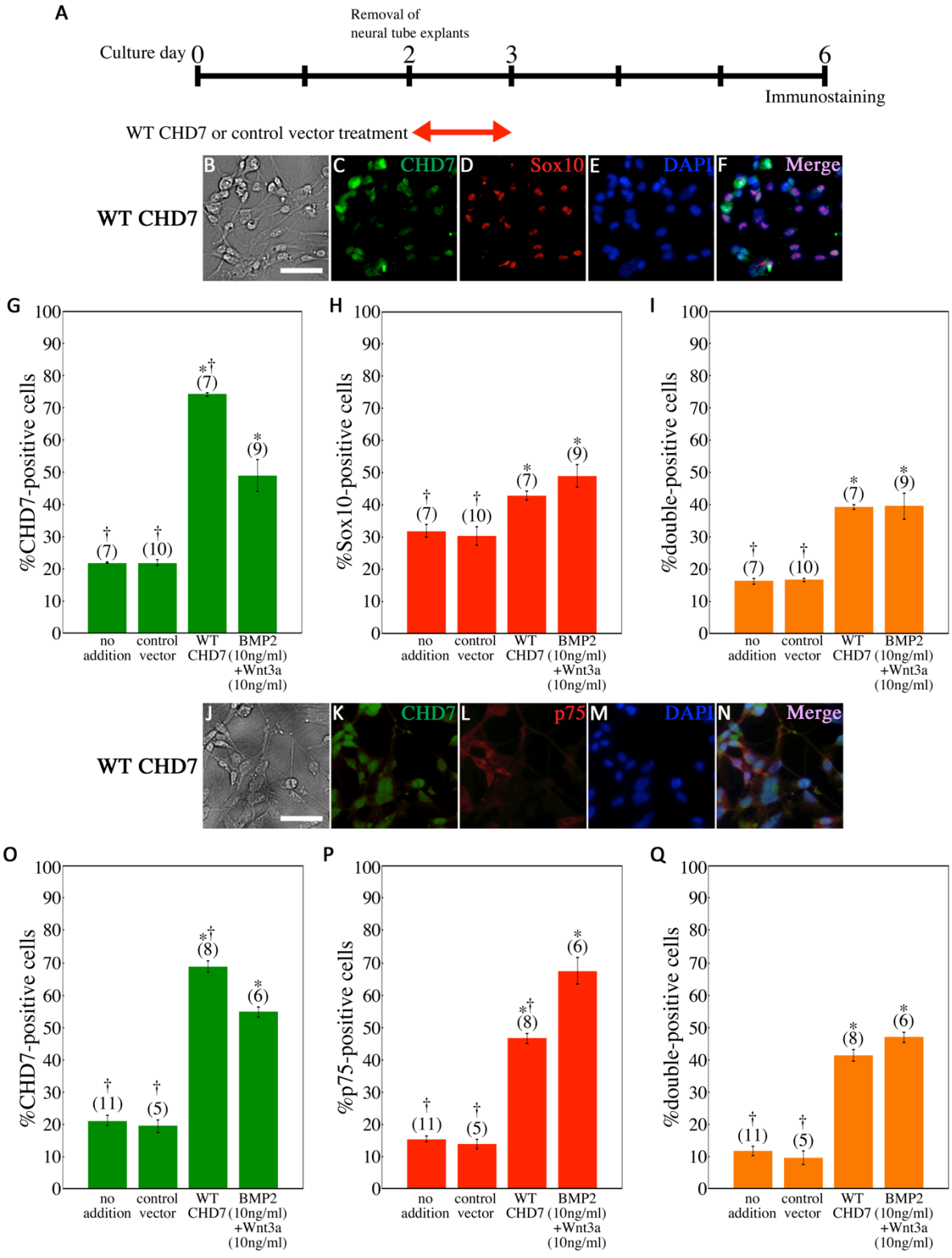

Fig. 1.8 Effects of the WT CHD7 expression vectors on the maintenance of the undifferentiated state. **(A)** After removal of neural tube explants, mouse trunk neural crest cells were exposed to the WT CHD7 expression vectors from 2 days to 3 days in culture. Immunostaining with anti-CHD7 and anti-Sox10 or with anti-CHD7 and anti-p75 was performed on culture day 6. **(B)** Bright-field image in the presence of the WT CHD7 expression vectors. **(C)** Anti-CHD7-positive cells in the same field as (B). **(D)** Anti-Sox10-positive cells in the same field as (B). **(E)** DAPI nuclear stain of the same field as (B). **(F)** Merged image of (C-E). **(G)** Percentage of cells expressing CHD7 per total cells in a neural crest cell colony (each colony was derived from a neural tube explant). **(H)** Percentage of cells expressing Sox10 per total cells in a neural crest cell colony. **(I)** Percentage of cells expressing both CHD7 and Sox10 per total cells in a neural crest cell colony. **(J)** Bright-field image in the presence of the WT CHD7 expression vectors. **(K)** Anti-CHD7-positive cells in the same field as (J). **(L)** Anti-p75-positive cells in the same field as (J). **(M)** DAPI nuclear stain of the same field as (J). **(N)** Merged image of (K-M). **(O)** Percentage of cells expressing CHD7 per total cells in a neural crest cell colony. **(P)** Percentage of cells expressing p75 per total cells in a neural crest cell colony. **(Q)** Percentage of cells expressing both CHD7 and p75 per total cells in a neural crest cell colony. *, $p < 0.05$ (Student's *t*-test) compared to the untreated cultures. †, $p < 0.05$ (Student's *t*-test) compared to the BMP2/Wnt3a-treated cultures. Data are expressed as mean ± SEM of separate counts of 5-11 colonies (the number in a parenthesis on each bar). Scale Bars = 50 μm.

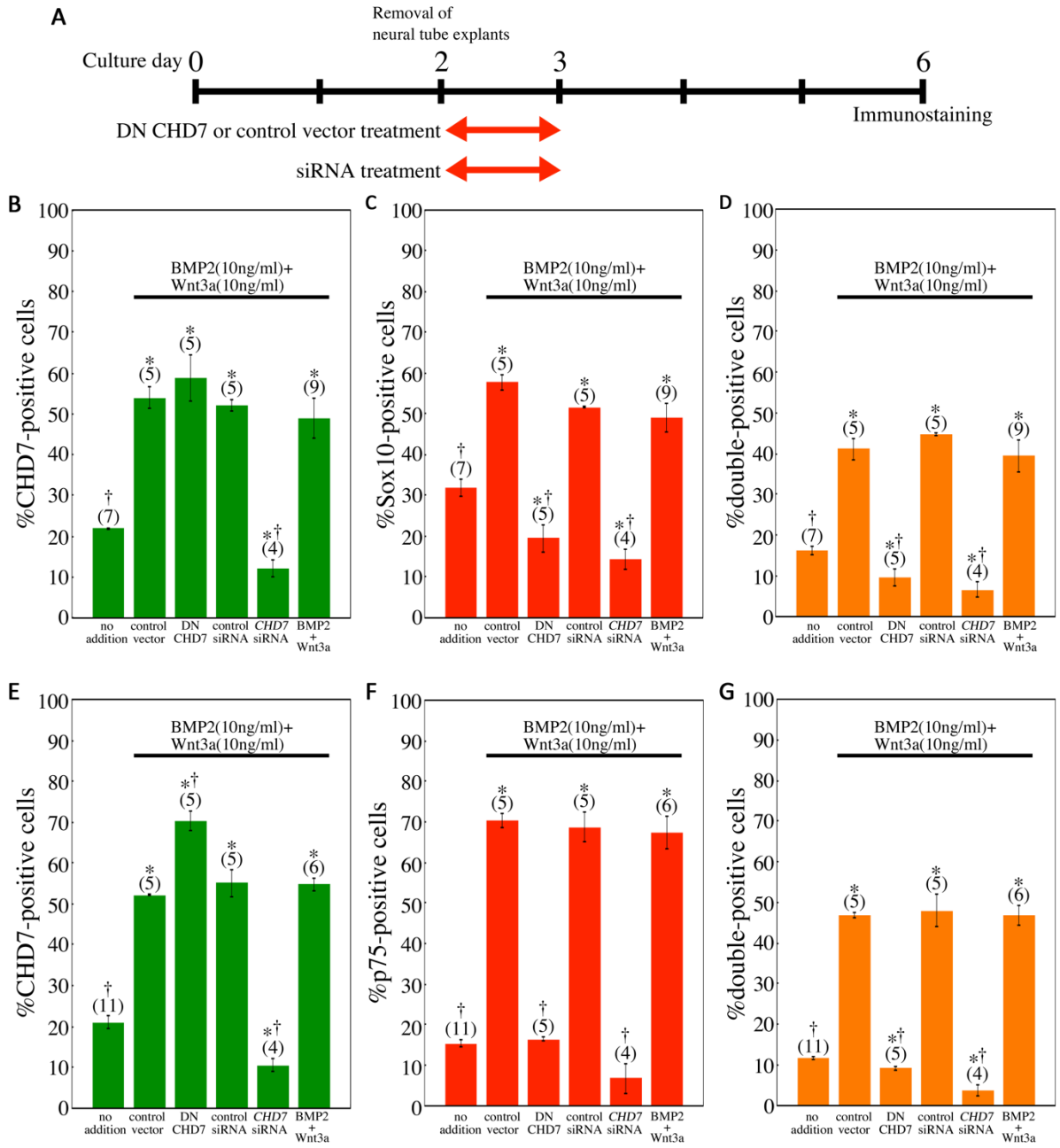

Fig. 1.9 Effects of the DN CHD7 expression vectors or *CHD7* siRNA on the maintenance of the undifferentiated state. **(A)** After removal of neural tube explants, mouse trunk neural crest cells were exposed to BMP2 and Wnt3a from 2 days to 6 days in culture. The DN CHD7 expression vectors or *CHD7* siRNA were applied from 2 days to 3 days in culture. Immunostaining with anti-CHD7 and anti-Sox10 or with anti-CHD7 and anti-p75 was performed on culture day 6. **(B)** Percentage of cells expressing CHD7 per total cells in a neural crest cell colony (each colony was derived from a neural tube explant). **(C)** Percentage of cells expressing Sox10 per total cells in a

neural crest cell colony. **(D)** Percentage of cells expressing both CHD7 and Sox10 per total cells in a neural crest cell colony. **(E)** Percentage of cells expressing CHD7 per total cells in a neural crest cell colony. **(F)** Percentage of cells expressing p75 per total cells in a neural crest cell colony. **(G)** Percentage of cells expressing both CHD7 and p75 per total cells in a neural crest cell colony. *, $p < 0.05$ (Student's *t*-test) compared to the untreated cultures. †, $p < 0.05$ (Student's *t*-test) compared to the BMP2/Wnt3a-treated cultures. Data are expressed as mean ± SEM of separate counts of 4-11 colonies (the number in a parenthesis on each bar).

Proliferation and apoptosis of mouse trunk neural crest cells by treatment with BMP2/Wnt3a or the WT CHD7 expression vectors

Since the number of the undifferentiated neural crest cells was significantly increased by treatment with BMP2 (10 ng/ml) /Wnt3a (10 ng/ml) or the WT CHD7 expression vectors, we examined the effects of these factors on the proliferation of mouse trunk neural crest cells using BrdU incorporation method. The percentage of BrdU-incorporated cells was increased by treatment with BMP2 (10 ng/ml) /Wnt3a (10 ng/ml) or the WT CHD7 expression vectors on culture day 6 (Fig. 1.10K). Furthermore, these treatments increased the proportion of BrdU-incorporated cells per total Sox10- or p75-expressing cells (Fig. 1.10A-E and L). The DAPI nuclear-staining experiments showed that almost no cell death occurs under treatment with BMP2 (10 ng/ml) /Wnt3a (10 ng/ml) or the WT CHD7 expression vectors. Therefore, we measured apoptosis in these culture conditions on culture day 6. No significant differences of the proportion of apoptotic cell death were found among the culture conditions examined (Fig. 1.10M). Moreover, no cells expressing both caspase-3 and Sox10 (Fig. 1.10F-J) or both caspase-3 and p75 were observed under the

culture conditions examined. BMP2/Wnt3a signaling or CHD7 is likely to promote the proliferation of undifferentiated mouse trunk neural crest cells.

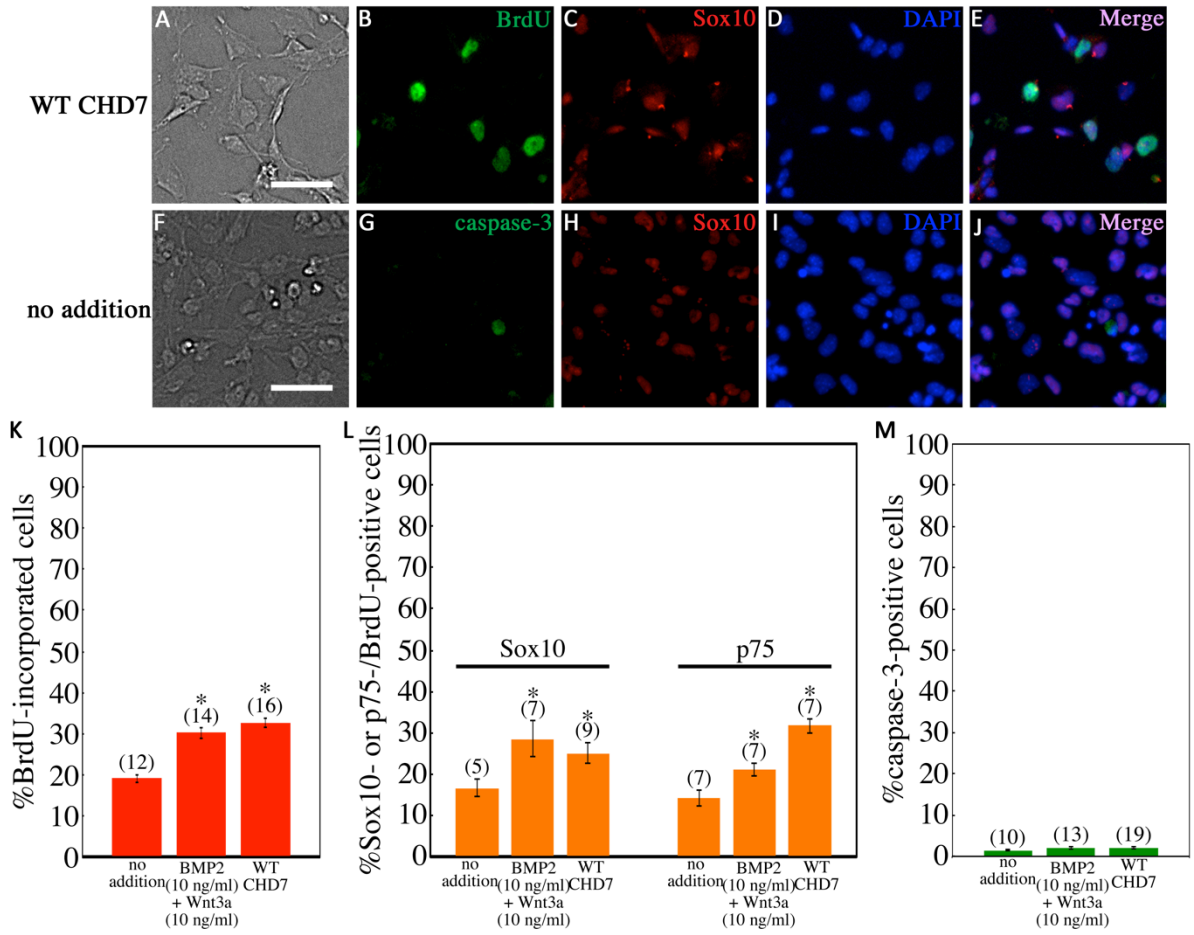

Fig. 1.10 Proliferation and apoptosis of mouse trunk neural crest cells. After removal of neural tube explants, mouse trunk neural crest cells were exposed to BMP2 and Wnt3a from 2 days to 6 days in culture. The WT CHD7 expression vectors were applied from 2 days to 3 days in culture. BrdU incorporation and the double-labeling with anti-Sox10 and anti-BrdU or with anti-p75 and anti-BrdU were carried out on culture day 6. The double-staining with anti-Sox10 and anti-caspase-3 or with anti-p75 and anti-caspase-3 was also performed on culture day 6. **(A)** Bright-field image in the presence of the WT CHD7 expression vectors. **(B)** BrdU-labeled cells in the same field as (A). **(C)** Anti-Sox10-positive cells in the same field as (A). **(D)** DAPI nuclear stain of the same field as (A). **(E)** Merged image of (B-D). **(F)** Bright-field image of an untreated culture. **(G)** Caspase-3-labeled

cells in the same field as (F). **(H)** Anti-Sox10-positive cells in the same field as (F). **(I)** DAPI nuclear stain of the same field as (F). **(J)** Merged image of (G-I). **(K)** Percentage of BrdU-incorporated cells per total cells in a neural crest cell colony (each colony was derived from a neural tube explant). **(L)** Percentage of anti-Sox10- or anti-p75-positive cells that incorporated BrdU per total Sox10- or p75-expressing cells in a neural crest cell colony. **(M)** Percentage of anti-caspase-3-positive cells per total cells in a neural crest cell colony. *, $p < 0.05$ (Student's *t*-test) compared to the untreated cultures. Data are expressed as mean ± SEM of separate counts of 5-19 colonies (the number in a parenthesis on each bar). Scale Bars = 50 μm.

Actions of CHD7 and BMP/Wnt signaling on the maintenance of the multipotency of mouse trunk neural crest cells

We showed here that CHD7 was expressed in undifferentiated mouse trunk neural crest cells and involved in the maintenance of the undifferentiated state. Since undifferentiated neural crest cells are likely to be multipotential, CHD7 and BMP2/Wnt3a may participate in maintaining the multipotency of mouse trunk neural crest cells. It has been known that multipotent trunk neural crest cells can differentiate into smooth muscle cells, neurons, and glia [47]. Therefore, we investigated whether or not the activation of CHD7 or BMP2/Wnt3a signaling triggers the increase in the number of multipotent mouse trunk neural crest cells that differentiate into smooth muscle cells, neurons, and glia. The trunk neural crest cells were treated with the WT CHD7 expression vectors or with BMP2 (10 ng/ml) /Wnt3a (10 ng/ml) and clonal cultures were subsequently performed in the presence or absence of 10 ng/ml FGF2 (Fig. 1.11A). FGF2 was required for glial differentiation in clonal cultures [40, 44]. Four types of clones appeared in the absence of FGF2: clones

containing both smooth muscle cells and neurons, clones containing either smooth muscle cells or neurons, and clones containing neither smooth muscle cells nor neurons (Fig. 1.11B-D). Furthermore, three types of clones were observed in the presence of FGF2: clones containing both smooth muscle cells and glia, clones containing smooth muscle cells only, and clones containing neither smooth muscle cells nor glia (Fig. 1.11F and G). The addition of WT CHD7 expression vectors or BMP2 (10 ng/ml) /Wnt3a (10 ng/ml) significantly increased the proportion of clones consisting of both smooth muscle cells and neurons or both smooth muscle cells and glia that originated from the multipotent trunk neural crest cells (Fig. 1.11E and H). These results suggest that BMP2/Wnt3a signaling or CHD7 profoundly participate in the maintenance of the multipotency of mouse trunk neural crest cells. Thus, cells expressing CHD7 and Sox10 or expressing CHD7 and p75 observed in mouse trunk neural crest cell cultures, the number of which was increased by BMP2/Wnt3a treatment, may be NCSCs.

Expression of CHD7 in mouse adult DRG and adult sciatic nerve

Adult DRG and adult sciatic nerves have been known to contain NCSCs expressing Sox10 and/or p75 [14-17]. Therefore, we analyzed the expression of CHD7, Sox10, and p75 in adult DRG and adult sciatic nerves. Cells expressing CHD7, Sox10, or p75 were observed in the adult DRG (Fig. 1.12A-J) and in the adult sciatic nerves (Fig. 1.12K-T). Moreover, the double-positive cells were found in any of tissues examined (arrowheads in Fig. 1.12).

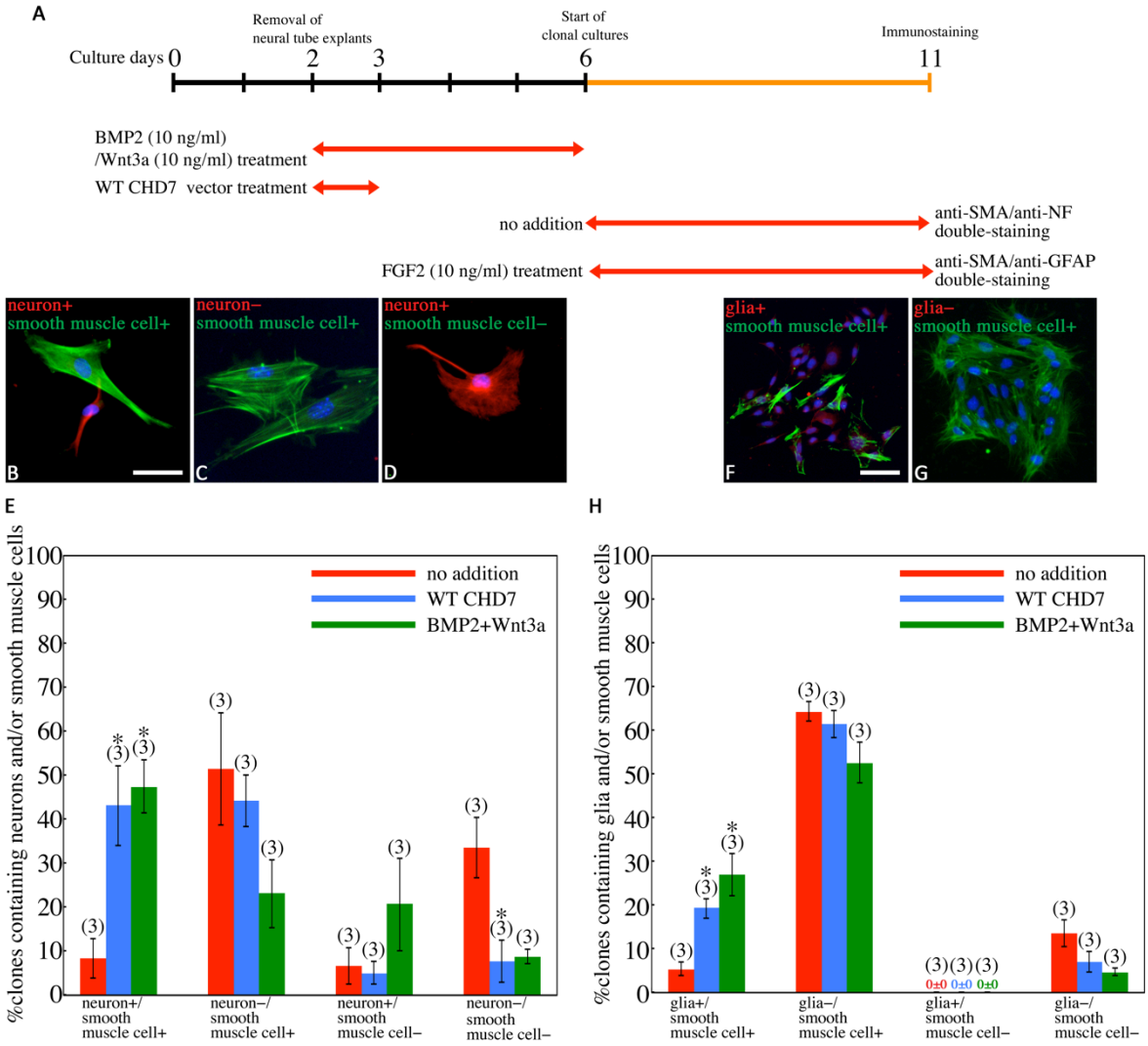

Fig. 1.11 Effects of the WT CHD7 expression vectors and BMP2/Wnt3a on the maintenance of the multipotency. **(A)** After removal of neural tube explants, mouse trunk neural crest cells were exposed to BMP2 and Wnt3a from 2 days to 6 days in culture. The WT CHD7 expression vectors were applied from 2 days to 3 days in culture. The clonal cultures were started on culture day 6. Immunostaining with anti-SMA and anti-NF or with anti-SMA and anti-GFAP was performed on culture day 11. In clonal cultures, FGF2 was added to the medium to stimulate the differentiation of anti-GFAP-positive glial cells. **(B)** A clone containing both anti-SMA (green)- and anti-NF (red)-positive cells in the presence of BMP2 and Wnt3a. **(C)** A clone containing anti-SMA-positive cells only in the presence of BMP2 and Wnt3a. **(D)** A clone containing anti-NF -positive cells only in the presence of BMP2 and Wnt3a. DAPI nuclear stain (blue). **(E)** Percentage of clones containing

cells expressing SMA and/or NF per total number of neural crest cell clones under various culture conditions. **(F)** A clone containing both anti-SMA (green)- and anti-GFAP (red)-positive cells in the presence of WT CHD7 expression vectors. **(G)** A clone containing anti-SMA-positive cells only in the presence of WT CHD7 expression vectors. DAPI nuclear stain (blue). **(H)** Percentage of clones containing cells expressing SMA and/or GFAP per total number of neural crest cell clones under various culture conditions. *, $p < 0.05$ (Student's *t*-test) compared to the untreated cultures. Data are expressed as mean ± SEM of separate counts of 3 independent experiments (the number in a parenthesis on each bar). Scale Bars = 50 μm.

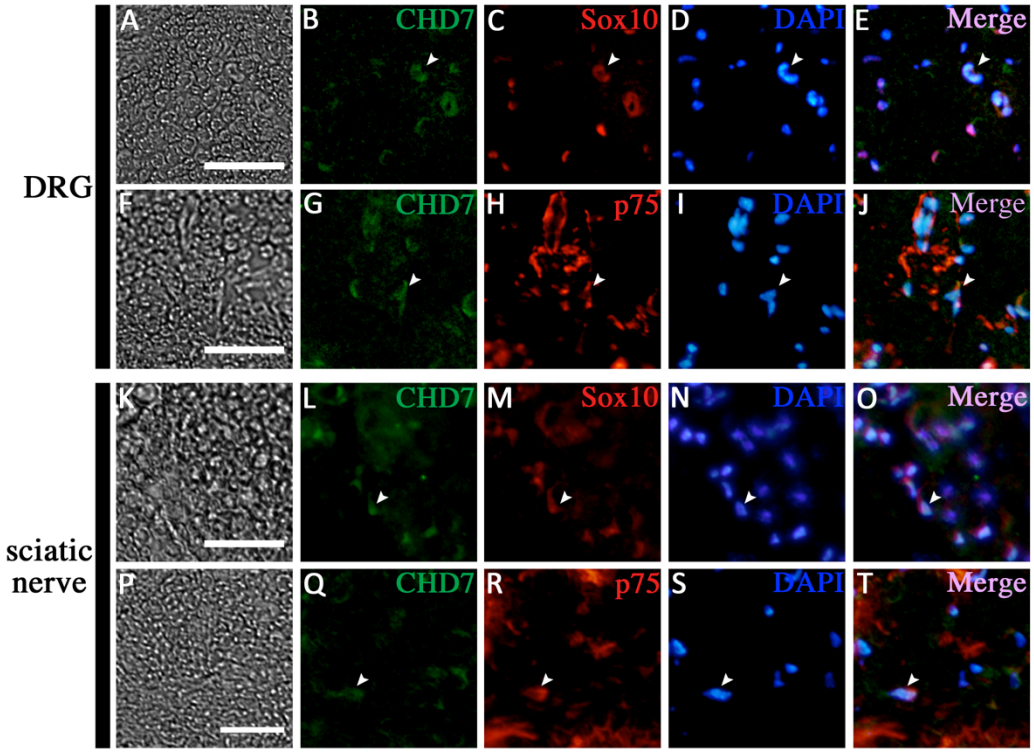

Fig. 1.12 Expression patterns of CHD7, Sox10, or p75 in DRG or sciatic nerve of adult mice.

(A-J) Transverse sections of DRG in a 12-week old mouse. **(A)** Bright-field image. **(B)** Expression pattern of CHD7 in the same field as (A). **(C)** Expression pattern of Sox10 in the same field as (A). **(D)** DAPI nuclear stain of the same field as (A). **(E)** Merged image of (B-D). **(F)** Bright-field image. **(G)** Expression pattern of CHD7 in the same field as (F). **(H)** Expression pattern of p75 in the same field as (F). **(I)** DAPI nuclear stain of the same field as (F). **(J)** Merged image of (G-I). **(K-T)** Transverse sections of sciatic nerve in a 12-week old mouse. **(K)** Bright-field image. **(L)** Expression pattern of CHD7 in the same field as (K). **(M)** Expression pattern of Sox10 in the same field as (K). **(N)** DAPI nuclear stain of the same field as (K). **(O)** Merged image of (L-N). **(P)** Bright-field image. **(Q)** Expression pattern of CHD7 in the same field as (P). **(R)** Expression pattern of p75 in the same field as (P). **(S)** DAPI nuclear stain of the same field as (P). **(T)** Merged image of (Q-S). Arrowheads show cells expressing both CHD7 and Sox10 or both CHD7 and p75. Scale Bars = 20 μm.

Discussion

In the present study, we analyzed roles of a chromatin remodeler, CHD7 [25, 48, 49] and BMP/Wnt signaling in maintaining the multipotency of mouse trunk neural crest cells. Chromatin remodeling plays important roles in development and differentiation [50]. It has been shown that CHD7 controls the expression of genes that characterize ES cells [25] and is involved in the induction of neural crest cells [21], which show multipotency like ES cells. Immunohistochemistry using mouse embryos showed that CHD7 was expressed in undifferentiated trunk neural crest cells containing Sox10, which participates in the maintenance of the undifferentiated state of neural crest cells [9], and p75, another marker of undifferentiated neural crest cells [20]. Further, CHD7 expression was found in the dorsal neural tube. These *in vivo* data are consistent with the results of a previous study [21].

In mouse trunk neural crest cell cultures, the number of Sox10- or p75-positive undifferentiated neural crest cells decreased as the culture progressed. Similarly, CHD7 expression was also suppressed over time. These results suggest the hypothesis that CHD7 may participate in the maintenance of the undifferentiated state of neural crest cells. This hypothesis was examined by experiments using BMP and Wnt proteins. Kléber et al. (2005) [31] has shown that undifferentiated neural crest cells expressing Sox10 and p75 are maintained by combined treatment with BMP2 (10 ng/ml) and Wnt1 (unknown concentrations). In this study, BMP/Wnt treatment maintained CHD7 expression as well as Sox10/p75 expression. Thus, it is conceivable that CHD7 not only affects neural crest induction but also plays important roles in the maintenance of the undifferentiated state of mouse trunk neural crest cells.

Wnt1 and Wnt3a are expressed in partially overlapping domains in the dorsal neural tube in which neural crest cells are formed [41]. When Wnt3a was added to mouse trunk neural crest cell cultures with BMP2, the expression of CHD7, Sox10, and p75 was maintained more effectively than the addition of Wnt1. Moreover, a high concentration of Wnt3a (100 ng/ml) independently maintained the expression of CHD7, Sox10, and p75, similar to the case with 10 ng/ml BMP and 10 ng/ml Wnt3a. This effect was unchanged even in the presence of noggin or chordin. These data suggest that the activation of Wnt signaling is a key requisite for the maintenance of CHD7 expression and thus for the maintenance of the undifferentiated state of neural crest cells, and that BMP signaling plays supportive roles in the maintenance of the undifferentiated state of these cells, as shown in the maintenance of the undifferentiated state of ES cells [51-53]. The addition of BIO, instead of Wnt, to neural crest cell cultures also maintained the undifferentiated state. Furthermore, the effects of BMP2 and Wnt3a were inhibited by the DN β-catenin or DN TCF expression vectors. These results suggest that the Wnt/β-catenin pathway is essential to the maintenance of the undifferentiated state of mouse trunk neural crest cells.

Wnt signaling plays important roles in neural crest induction [54]. Neurons derived from the proximal ganglion of cranial nerve IX are absent in the mutant mouse embryos lacking both Wnt1 and Wnt3a [55]. Further, β-catenin mutant mouse embryos lack melanocytes and sensory neurons [56]. These *in vivo* data have shown that the Wnt/β-catenin pathway participates in neural crest induction and differentiation [57]. In addition, it has been known that BMP signaling is essential for neural crest induction [4] and BMP2 is especially required for migration of mouse neural crest cells [58]. In the present study, BMP2 and/or Wnts also promoted sensory neurogenesis of mouse trunk neural crest cells. Thus, it is possible that BMP/Wnt signaling affect multiple aspects of neural crest

development such as induction, migration, differentiation, the maintenance of the undifferentiated state.

When mouse trunk neural crest cell cultures were treated with the WT CHD7 expression vectors, the undifferentiated state of the trunk neural crest cells was maintained, similar to the case with BMP2 (10 ng/ml) /Wnt3a (10 ng/ml) treatment. The treatment with the DN CHD7 expression vectors or *CHD7* siRNA significantly inhibited the effects of BMP2/Wnt3a. It is conceivable that CHD7 participates in the maintenance of the undifferentiated state of mouse trunk neural crest cells as well as in neural crest induction [21], similar to the case with BMP/Wnt signaling.

BrdU-incorporated experiments showed that the proliferation of undifferentiated mouse trunk neural crest cells were significantly promoted by the treatment with BMP2/Wnt3a or WT CHD7 expression vectors. On the other hand, any selective cell death was not found in these treatments. Thus, the maintenance of the undifferentiated state of the trunk neural crest cells may be due to the promotion of the proliferation of the undifferentiated neural crest cells by BMP2/Wnt3a signaling and the chromatin remodeler.

The maintenance of the undifferentiated state of mouse trunk neural crest cells may enable the maintenance of the multipotency of these cells. In fact, the results of clonal cultures showed that multipotent cells were increased by the addition of WT CHD7 expression vectors or BMP2/Wnt3a. Furthermore, CHD7-containing cells expressing Sox10 or p75 were observed in the DRG and sciatic nerves of adult mice that had NCSCs [14, 15]. These results suggest that CHD7 as well as Sox10 participates in the maintenance of the multipotency of neural crest cells and conduct them to mouse NCSCs expressing p75. Taken together, the present results suggest the possibility that BMP2/Wnt3a signaling and CHD7 play essential roles in the maintenance of the multipotency of mouse trunk neural crest cells, leading to the formation of mouse NCSCs (Fig. 1.13).

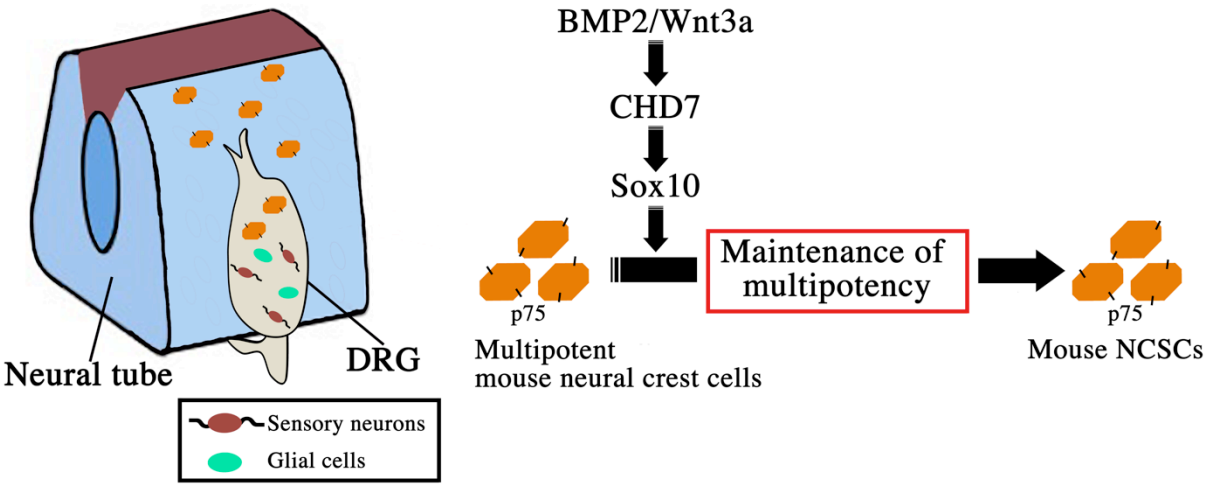

Fig. 1.13 Involvement of CHD7 and BMP2/Wnt3a signaling in the formation of mouse NCSCs.

CHD7, which is activated by BMP2/Wnt3a signaling, maintains the multipotency of mouse neural crest cells through the promotion of Sox10 expression and leads to the formation of mouse NCSCs expressing p75.

Chapter II

Direct control of FoxD3 expression by CHD7, Oct3/4, Sox2, and Nanog in the formation of mouse neural crest-derived stem cells

Introduction

Neural crest induction is initiated by BMPs/Wnts signaling at the neural plate border [3]. These signaling molecules induce the expression of neural crest inducer genes, *Msx1*, *Zic1*, and *Pax3/7* [6]. Furthermore, these transcriptional factors activate neural crest specifier genes such as *FoxD3*, *Sox9*, *Sox10*, and *Twist1* [7, 8]. Neural crest specifier genes participate in the generation of multipotent neural crest cells [47, 59, 60]. FoxD3 is also indispensable for the maintenance of pluripotency in ES cells [61, 62].

As described in Chapter I, some neural crest cells maintain their multipotency and form NCSCs in various tissues, including DRG, sciatic nerve, epidermis, cardiac outflow tract, and bone marrow [10-13]. We have shown that CHD7 as well as Sox10 plays important roles in the formation of mouse NCSCs and the activities of CHD7 and Sox10 are promoted by BMP2/Wnt3a treatment [63].

CHD7 has been known to interact with histone H3 methylated at lysine 4 in enhancer regions of target genes via its chromodomains [64, 65]. CHD7 regulates the activities of *Sox9* and *Twist1* by binding to H3K4me1 in the enhancer regions of the genes of these transcription factors in neural crest induction [21]. In addition, CHD7 and the products of the pluripotent stem cell-related genes, which contain *Oct3/4*, *Sox2*, and *Nanog*, colocalize at

CHD7 binding sites of target gene enhancers marked with H3K4me1 in ES cells [25]. Furthermore, it has been shown that neural crest cells and neural crest-derived cells express Oct3/4, Sox2, and Nanog [66, 67].

The data described above suggest that the interaction among CHD7, the neural crest inducer genes, the neural crest specifier genes, and the pluripotent stem cell-related genes may play essential roles in the formation of NCSCs (Fig. 2.1). However, nothing is known about their interactions in the formation of NCSCs. In the present study, therefore, we analyzed the roles of CHD7, neural crest inducer genes, neural crest specifier genes, and pluripotent stem cell-related genes in the formation of NCSCs. Data show that *FoxD3* activation by CHD7 and the products of pluripotent stem cell-related genes are required for the formation of mouse NCSCs.

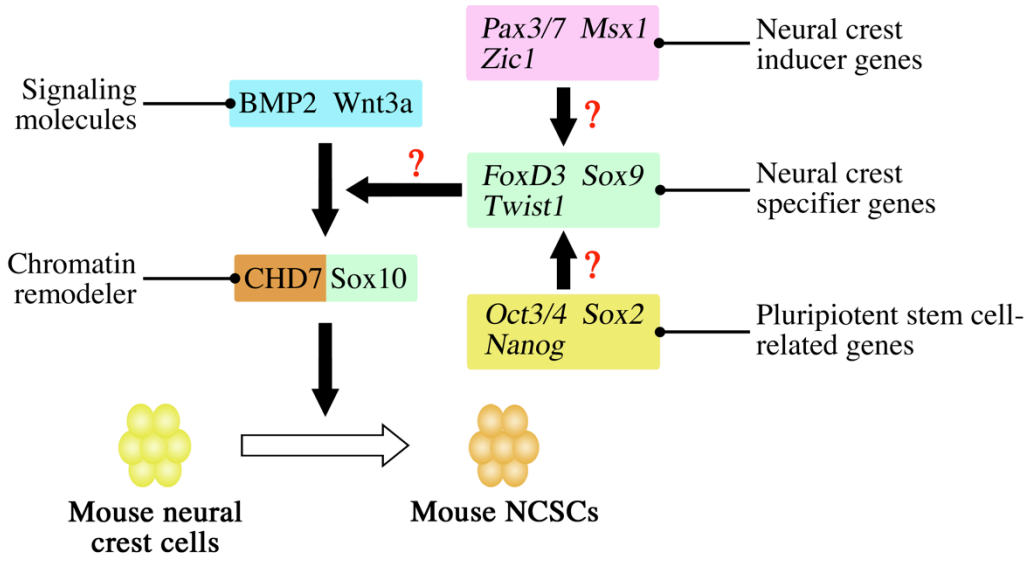

Fig. 2.1 Hypothesis for a regulatory gene cascade in the formation of mouse NCSCs. We have shown that BMP2/Wnt3a signaling activates *CHD7* and *Sox10* and that activation of these factors leads to the formation of mouse NCSCs [63]. Now, we propose a hypothesis that the products of neural crest specifier genes promote the expression of CHD7 and/or Sox10 and that neural crest inducer genes and/or pluripotent stem cell-related genes play important roles in the NCSCs formation through the activation of neural crest specifier genes.

Materials & Methods

Primary cultures

Primary cultures of mouse trunk neural crest cells were performed by using procedures described in Chapter I. Neural tubes isolated from E9.5 embryos were explanted into collagen-coated 35-mm culture dishes. The explants were scraped away with a tungsten needle after 48 h in culture, leaving the emigrated trunk neural crest cells on the substratum. The culture medium consisted of 85% α-MEM (Sigma), 10% FBS (GE Healthcare Life Sciences), 5% CEE, and 50 μg/ml gentamicin (Sigma). BMP2 (R&D Systems) and Wnt3a (R&D Systems) were added to the medium at a concentration of 10 ng/ml.

Transfection of CHD7 expression vector or siRNAs

Mouse trunk neural crest cells were transfected with 1 μg of pcDNA3.1 encoding the human WT CHD7 and a Flag-6×His tag (a gift from Dr. J. Wysocka, Stanford University) [21] or with siRNAs for 24 h immediately after the removal of the neural tubes, using Lipofectamine 2000 (Invitrogen). The siRNA duplexes for *FoxD3*, *Sox9*, *Twist1*, *CHD7*, *Oct3/4*, *Sox2*, *Nanog*, *Setd7*, *MLL1*, *Setd1a*, *ESET*, and *Suv39h1* were designed on the basis of their sequences published online [GenBank Accession Nos. NM01425, NM011448, NM011658, NM001081417, NM 001252452, NM011443, AB093574, NM080793, NM001081049, NM178029, NM018877, NM011514]. All siRNA sequences are listed in Table 2.1. pcDNA3.1 (Invitrogen) and Stealth™ RNAi Negative Control Medium GC Duplex #2 (Invitrogen) was used as the control.

Table 2.1. List of siRNA sequences

Gene	Sequence (5' to 3')
FoxD3	UUCACCAGGCUGUUCUUGGGCUUGU
Sox9	CCAGCAAGAACAAGCCACACGUCAA
Twist1	CCAGGUACAUCGACUUCCUGUACCA
CHD7	CAGGCUCAAGCUAGAUGCCACAGAA
Oct3/4	CCGGAAGAGAAAGCGAACUAGCAUU
Sox2	UUUAUAAUCCGGGUGCUCCUUCAUGs
Nanog	UUAUAGCUCAGGUUCAGAAUGGAGG
Setd7	AAUGGAUCCAACACACUCCGUGUCG
MLL1	UUAUAUUGCGGCCACCAAACUUGGG
Setd1a	UUUGGCUGCAUUCUGGAAUGGCUUG
ESET	CCAAGCAGCUGACACUGAAAGCUUA
Suv39h1	AUUCAAUACGGACUCGUUUCUUGGG

All siRNA were designed by BLOCK-iT™ RNAi Designer

(http://rnaidesigner.thermofisher.com/rnaiexpress/).

Immunofluorescence

Immunostainings were performed as a described in Chapter I. Primary cultures of mouse trunk neural crest cells were fixed with 4% PFA for 1 h on ice. The cultures were immunostained with the primary antibodies for 16 h at 4°C and with the secondary antibodies for 1 h at room temperature. The antibodies are listed in Table 2.2. Finally, the cultures were nuclear-stained with 0.1 μg/ml DAPI (Dojindo). DAPI nuclear staining was important for counting the exact number of immunoreactive cells in the cultures and for judging cell death.

µChIP-qPCR

µChIP was performed by using a modification of the method described by Dahl and Collas (2008) [68] (Fig. 2.2). Mouse trunk neural crest cells were cross-linked by adding FA for 8 min at room temperature. The final concentration of FA was 1%. Cross-linked cells were washed with PBS containing 20 mM NaBu. The cell pellets were resuspended and lysed in lysis buffer [1% SDS, 10 mM EDTA, 50 mM Tris-HCl, pH 8.0, 20 mM NaBu, and protease inhibitor tablet (Complete Protease Inhibitor Mini EDTA-free, Roche)] for 5 min on ice. The lysate was diluted 5-fold with RIPA buffer (0.1% SDS, 1 mM EDTA, 10 mM Tris-HCl, pH 8.0, 150 mM NaCl, 0.5 mM EGTA, 0.1% Na-deoxycholate, 1% Triton X-100, and protease inhibitor) and sonicated using Advanced Sonifier 250A at output 2, duty cycle 60% for 6×10 s pulses each with a 2 min pause between pulses on ice. Chromatin fragments were incubated with 10 µl Protein G-coated paramagnetic beads for 2 h at 4°C that had been preincubated with 5-10 µg of the appropriate antibodies. Antibodies are listed in Table 2.2. The complexes were washed twice with RIPA buffer and once with TE, and were eluted in elution buffer (1% SDS, 20 mM Tris-HCl, pH 8.0, 50 mM NaCl, 5 mM EDTA, and 20 mM NaBu) from the beads by heating at 65°C with occasional vortexing. The cross-linking was reversed by incubation at 65°C overnight. DNA was purified by treatment with Proteinase K (0.2 mg/ml) and phenol/chloroform/isoamyl alcohol. Real-time PCR reactions were carried out using ABI7300. The primer sequences used for PCR are shown in Table 2.3.

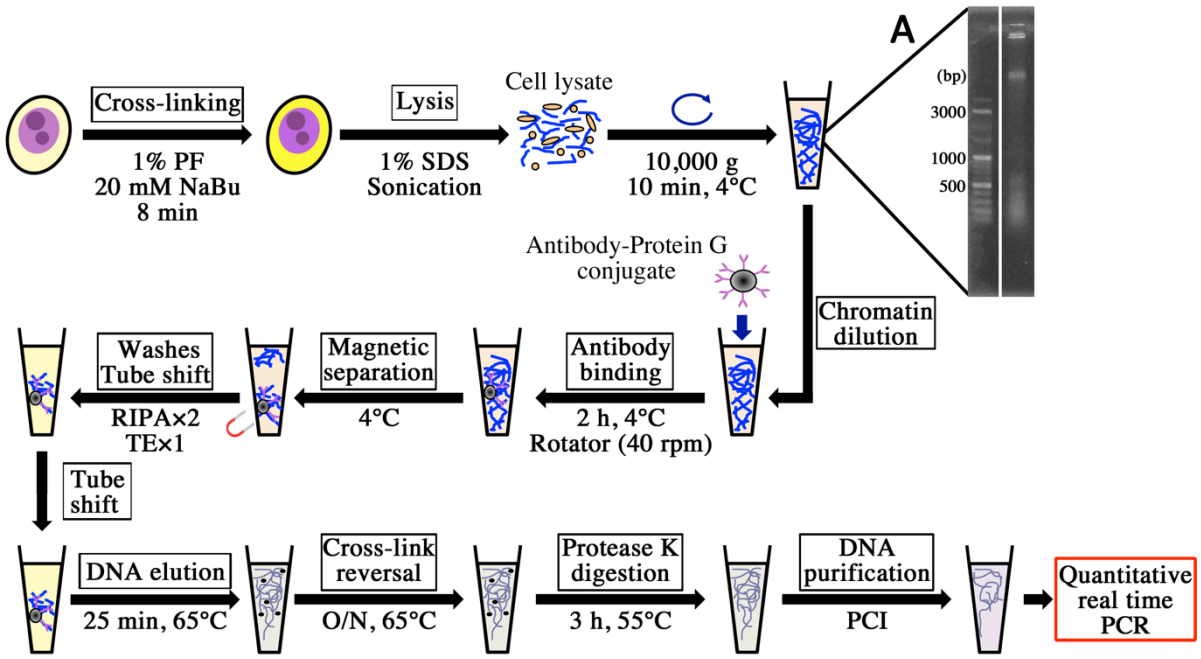

Fig. 2.2 Schematic diagram of the μChIP assay. **(A)** Agarose gel electrophoresis assessment of chromatin fragmentation. Chromatin derived from mouse trunk neural crest cells was fragmented by sonication. DNA isolated from these chromatin fragments was resolved in 1.5% agarose and stained with ethidium bromide. Most of the DNA fragments concentrated in the 200-700 bp.

Public data

ChIP-seq raw data were downloaded from Chromatin Regulator Cistrome (http://cistrome.org/cr/index.php) using accession GSM558674 [25] and from NCBI GEO (www.ncbi.nlm.nih.gov/gds) using accessions GSM1082340, GSM1082341, GSM1082342, GSM1082343, GSM307137, GSM307138, GSM307140, and GSM307155 [69, 70].

Table 2.2. Antibodies used for immunostaining and μChIP

Antibodies used for Immunofluorescence

Antigen/Conjugation	Dilution	Catalog number
Sox10 (rabbit polyclonal antibody)	1:100	MILLIPORE (AB5727)
CHD7 (goat polyclonal antibody)	1:100	Santa Cruz (sc-79207)
FoxD3 (5G9, mouse monoclonal IgG1)	1:300	Sigma (SAB5300098)
Alexa Fluor 488 (Donkey anti-Goat IgG)	1:500	Invitrogen (A-11055)
Alexa Fluor 488 (Donkey anti-Mouse IgG)	1:500	Invitrogen (A-21202)
Alexa Fluor 555 (Donkey anti-Rabbit IgG)	1:500	Invitrogen (A-31572)

Antibodies used for μChIP

Antigen	Amount	Catalog number
CHD7 (rabbit polyclonal antibody)	10 μg	Abcam (ab31824)
Oct3/4 (rabbit polyclonal antibody)	5 μg	Santa Cruz (sc-9081 X)
Sox2 (goat polyclonal antibody)	5 μg	Santa Cruz (sc-17320 X)
Nanog (D1G10, rabbit monoclonal IgG)	5 μl	Cell Signaling (8785)
Pax3/7 (rabbit polyclonal antibody)	5 μg	Santa Cruz (sc-25409 X)
Msx1 (rabbit polyclonal antibody)	5 μg	Santa Cruz (sc-15395 X)
Zic1 (rabbit polyclonal antibody)	5 μg	Sigma (HPA004098)

Table 2.3. Primers used for μChIP-qPCR

Primer name	Sequence (5' to 3')
FoxD3 mE1 fwd	GTTACCTCCTTTGCCCAGAA
FoxD3 mE1 rev	GTTGTGTAGAGAAAGGAGCATTTGAG
FoxD3 mE2 fwd	AGCAAGCCAGTCGCTAGCA
FoxD3 mE2 rev	GGGAATATCTAATGAGCTCGAGGAA
FoxD3 mE3 fwd	GCAGCCACTGGGTTTGCT
FoxD3 mE3 rev	ATGACGGCTGCGTGATGA
Sox9 E1 fwd	GCTCTCTTACAGAGGCCTTCCAA
Sox9 E1 rev	CTCACTGGCTTGTGTGGAGTCT
Sox9 E3 fwd	TCCCTCCGCCCCAACT
Sox9 E3 rev	GGGTACCAGCCCCATCTTCT
Sox10 D6 fwd	TCAAGCTGGGTGCTGAAATTT
Sox10 D6 rev	CCTGGATGCCAGCACAAAG
Sox10 D7 fwd	TCAAGCCAGCCATTGTTCCT
Sox10 D7 rev	GGGATCCGAGTCCTCGATAAG
Sox10 U3 fwd	GCGCGCGACGTTGAC
Sox10 U3 rev	AACACAATAGAGGGATTTGTTGCA

Identification of highly conserved genomic regions of mouse *FoxD3*

UCSC Genome Browser (http://genome.ucsc.edu) was used to identify highly conserved genomic regions of mouse *FoxD3*. The sequence reads were aligned to the mm9 assembly of the mouse genome. A BigWig file of the CHD7 ChIP-seq data set (GSM558674) was created by using SraTailor software (www.devbio.med.kyushu-u.ac.jp/sra_tailor/) [71] and the file was converted to WIG with the bigWigToWig program from UCSC. WIG files (GSM558674, GSM1082340,

GSM1082341, GSM1082342) were visualized by using the UCSC Genome Browser. We identified three highly conserved genomic regions of mouse *FoxD3*, mE1, mE2, and mE3. The conserved region in which the ChIP-seq peaks of CHD7, Oct3/4, Sox2, and Nanog overlapped was named mE1. mE2 and mE3 are homologous with chick *FoxD3* enhancer elements NC1 and NC2 [72], respectively. Highly conserved *cis*-regulatory regions of mouse *Sox9* and *Sox10* were visualized by using the UCSC Genome Browser.

Binding motif analysis

MEME-ChIP (http://meme-suite.org/tools/meme-chip) [73] was used to find *de novo* binding motifs of CHD7 with default parameters. We obtained ChIP-seq peak regions from a BED file of ChIP-seq data (GSM558674) and analyzed 500 bp of the genomic sequence centered on each peak declared by Schnetz et al. (2010) [25]. Nanog binding motifs were obtained by using the MotIV program contained in the ChIP-seq pipeline of the National Institute of Genetics (https://cell-innovation.nig.ac.jp/members/index_en.html). Binding motifs of Oct3/4, Sox2, Pax3/7, Msx1, and Zic1 were obtained from the JASPAR database (http://jaspar.genereg.net/cgi-bin/jaspar_db.pl). Based on the information of these binding motifs, binding sites of CHD7 and Nanog were predicted by using FIMO (http://meme-suite.org/tools/fimo) and of Oct3/4, Sox2, Pax3/7, Msx1, and Zic1 were anticipated by using the JASPAR database.

Results

FoxD3 and Sox9 control Sox10 expression

Since it has been known that Sox10, which is required for the formation of mouse NCSCs by BMP2/Wnt3a signaling [63], interacts with FoxD3, Sox9, and Twist1 in neural crest induction [8], we examined whether or not FoxD3, Sox9, and Twist1 affect Sox10 expression to form NCSCs. Mouse trunk neural crest cells were treated with *FoxD3*, *Sox9*, and *Twist1* siRNA (Fig. 2.3A). Whereas Sox10 expression was significantly suppressed by knocking down *FoxD3* and *Sox9* even under BMP2/Wnt3a-treated conditions (Fig. 2.3B-E, G), *Twist1* siRNA had no effect on Sox10 expression (Fig. 2.3G). Furthermore, no effects on CHD7 expression were evident in any of the siRNAs examined (Fig. 2.3F). These results indicate that FoxD3 and Sox9 promote Sox10 expression in the formation of mouse NCSCs.

CHD7, Oct3/4, Sox2, and Nanog directly bind to the highly conserved genomic regions of *FoxD3* in a BMP2/Wnt3a-dependent manner

The neural crest inducer genes *Pax3/7*, *Msx1*, and *Zic1* control the expression of neural crest specifier genes [6-8]. Furthermore, FoxD3 has been shown to maintain the pluripotency of ES cells by interacting with the pluripotent stem cell-related genes *Oct3/4*, *Sox2*, and *Nanog* [74, 75]. Therefore, we examined the binding of the neural crest inducer genes and the pluripotent stem cell-related genes to the *cis*-elements of *Sox9*, *Sox10*, and *FoxD3* by μChIP-qPCR analyses. We focused on two *cis*-regulatory elements (E1 and E3)

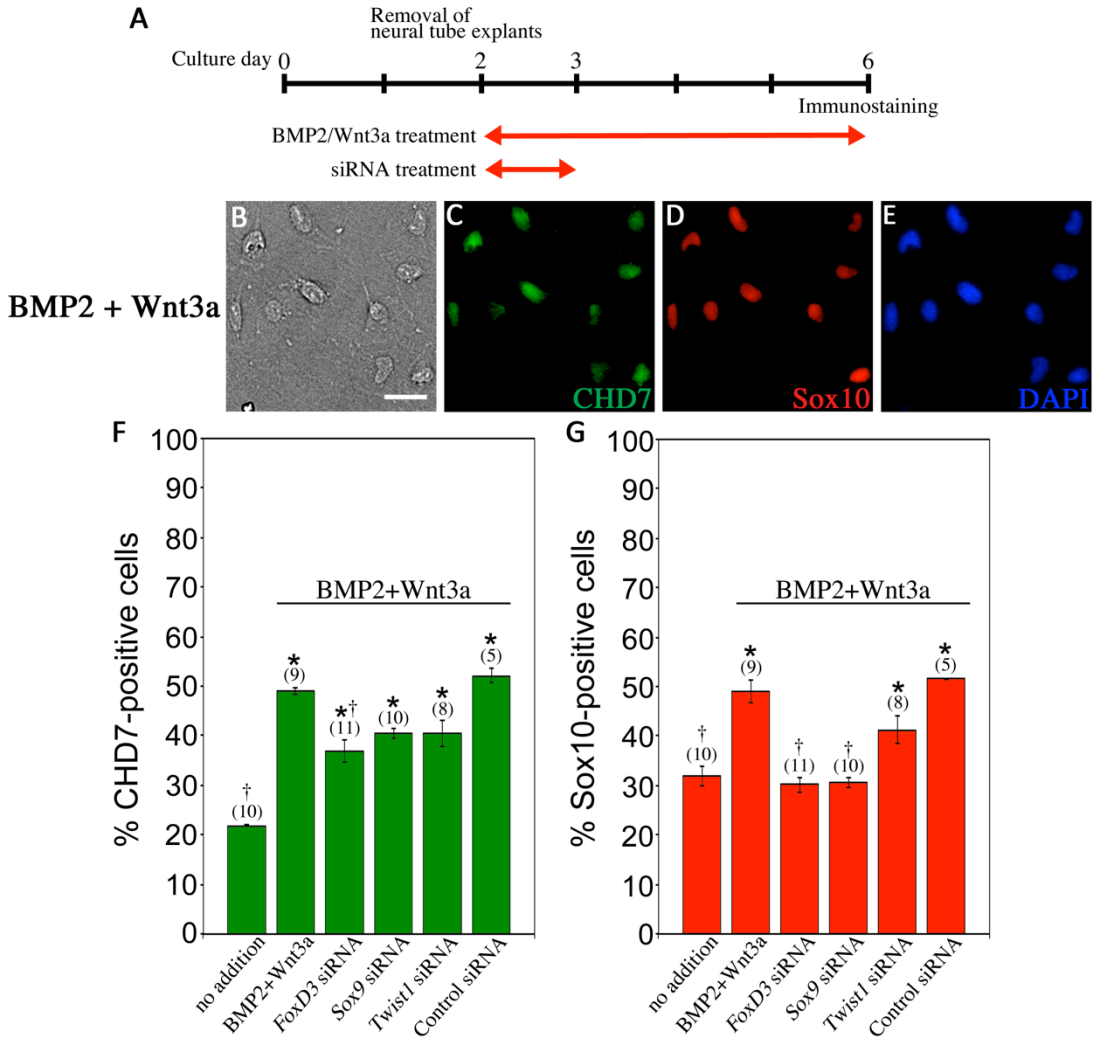

Fig. 2.3 Effects of *FoxD3*, *Sox9*, or *Twist1* siRNA on Sox10 and CHD7 expression in mouse trunk neural crest cells. **(A)** After removal of neural tube explants, mouse trunk neural crest cells were exposed to BMP2 and Wnt3a from 2 days to 6 days in culture. *Sox9*, *FoxD3*, or *Twist1* siRNA were applied from 2 days to 3 days in culture. Immunostaining with anti-CHD7 and anti-Sox10 was performed on culture day 6. **(B)** Bright-field image in the presence of BMP2 and Wnt3a. **(C)** Anti-CHD7-positive cells in the same field as (B). **(D)** Anti-Sox10-positive cells in the same field as (B). **(E)** DAPI nuclear stain of the same field as (B). **(F)** Percentage of cells expressing CHD7 per total cells in a neural crest cell colony (each colony was derived from a neural tube explant). **(G)** Percentage of cells expressing Sox10 per total cells in a neural crest cell colony. *, $p < 0.05$ (Student's *t*-test) compared to the untreated cultures. †, $p < 0.05$ (Student's *t*-test) compared to the

BMP2/Wnt3a-treated cultures. Data are expressed as mean ± SEM of separate counts of 5-11 colonies (the number in a parenthesis on each bar). Scale Bar = 50 μm.

---

of *Sox9* [21, 76] and three *cis*-regulatory elements (D6, D7, and U3) of *Sox10* [77, 78], which are active in mouse neural crest development (Fig. 2.4B, C). However, no regulatory elements have been identified in mouse *FoxD3*. Using the UCSC Genome Browser, therefore, we examined the genomic regions of *FoxD3* conserved among vertebrates including mouse, rat, human, opossum, chick, *X_tropicalis*, and zebrafish. Three regions, localized at 14 kb, 54 kb, and 143 kb upstream of the *FoxD3* gene, were found and were named mE1, mE2, and mE3, respectively (Fig. 2.4A). The mE2 and mE3 regions are homologous to the *cis*-regulatory regions, NC1 and NC2, identified in the chicken [72]. Previous ChIP-seq analyses using mouse ES cells [25, 69] showed direct binding of CHD7, Oct3/4, Sox2, and Nanog to the mE1 (Fig. 2.4A).

We performed μChIP-qPCR assays in mouse trunk neural crest cell cultures toward these eight *cis*-elements, using CHD7, Oct3/4, Sox2, Nanog, Pax3/7, Msx1, and Zic1 antibodies. μChIP assays indicated noticeable BMP2/Wnt3a-dependent enrichment of CHD7, Oct3/4, Sox2, and Nanog at mE1, mE2, and/or mE3 of *FoxD3* (Fig. 2.5). However, no significant enrichment was detected at the *Sox9* and *Sox10 cis*-elements for the products of pluripotent stem cell-related genes (Fig. 2.6B-D and 2.7B-D). CHD7 bound to the *Sox9* and *Sox10 cis*-elements in a BMP2/Wnt3a-independent manner (Fig. 2.6A and 2.7A). Whereas Pax3/7 bound to the *cis*-elements of *FoxD3* under the control condition only (Fig. 2.8A), this transcription factor showed binding activities to the *Sox9* and *Sox10 cis*-elements regardless of the presence or absence of BMP2/Wnt3a (Fig. 2.9A and 2.10A). No binding activities of Msx1 (Fig. 2.8B, 2.9B, and 2.10B) and Zic1 (Fig. 2.8C, 2.9C, and 2.10C) were found in any

of the *cis*-elements examined. These data suggest that CHD7, Oct3/4, Sox2, and Nanog bind directly to the *FoxD3* conserved elements in mouse NCSC formation (Fig. 2.11).

Based on the previous data of ChIP-seq, we found *de novo* binding motifs of CHD7 and Nanog. Using MEME-ChIP, six binding motifs were found in the CHD7 data set shown by Schnetz et al. (2010) [25] (Fig. 2.12A, 2.13A, and 2.14A). Using MotIV program, three binding motifs were obtained in the Nanog data set shown by Marson et al. (2008) [69] (Fig. 2.12A, 2.13A, and 2.14A). Binding motifs of Oct3/4, Sox2, Pax7, Msx1, and Zic1 were obtained from the JASPAR database. Judging from the information on binding motifs, we defined putative binding sites of CHD7, Sox2, Nanog, and Pax7 within *cis*-elements of *FoxD3*, *Sox9*, and *Sox10* (Fig. 2.12B-D, 2.13B, C, and 2.14B, C) and binding sites of Oct3/4, Msx1, and Zic1 within *FoxD3* and *Sox10 cis*-elements (Fig. 2.12B-D and 2.14B, C). These data are consistent with the present results of the μChIP-qPCR assays.

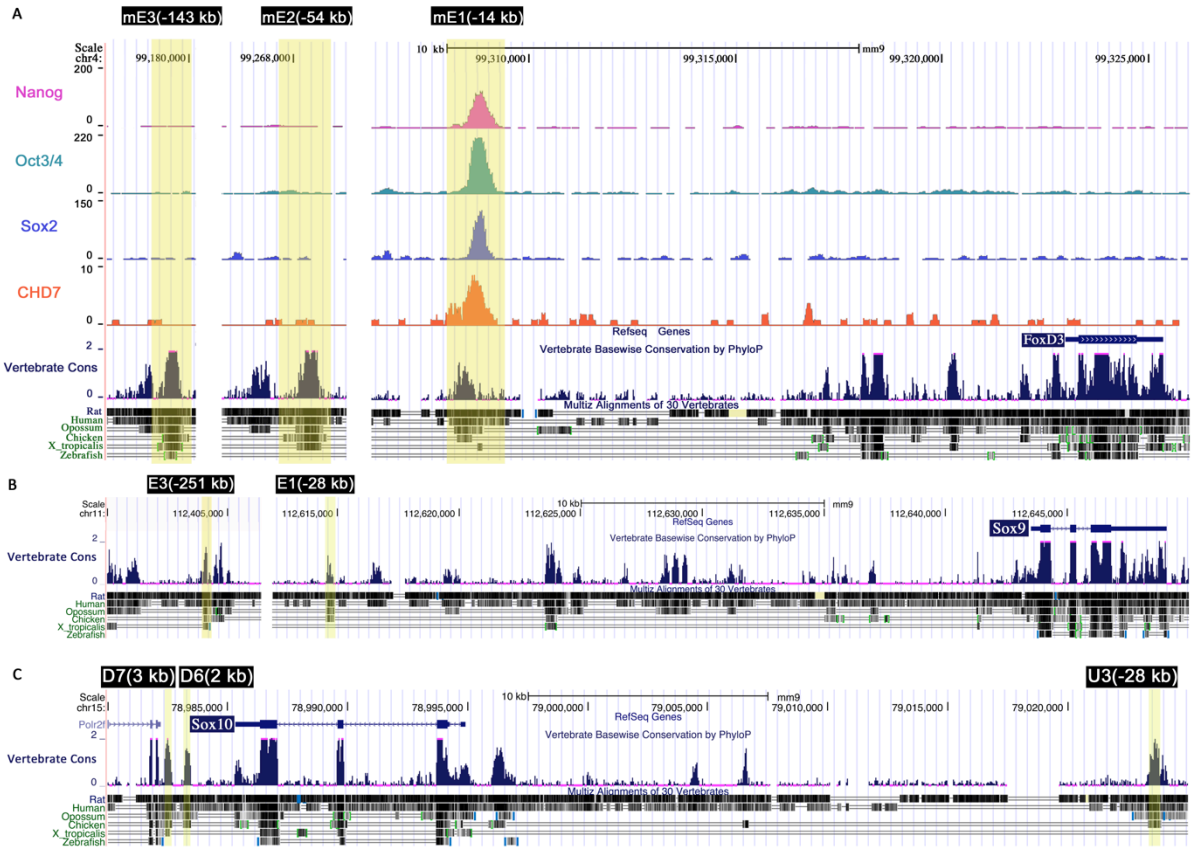

Fig. 2.4 Highly conserved genomic regions of mouse *FoxD3*, *Sox9*, and *Sox10*. **(A)** Schematic diagram showing comparative genomic analysis and ChIP-seq signals around mouse *FoxD3* using the UCSC genome browser. Rat, human, opossum, chicken, *X_tropicalis*, zebrafish *FoxD3* genomic sequences were compared. Three conserved regions (yellow) were named mE1, mE2, and mE3, respectively. **(B)** Schematic diagram showing comparative genomic analysis around mouse *Sox9*. *Sox9 cis*-regulatory elements, E1 and E3, were indicated by yellow. **(C)** Schematic diagram showing comparative genomic analysis around mouse *Sox10*. *Sox10 cis*-regulatory elements, D6, D7, and U3, were indicated by yellow.

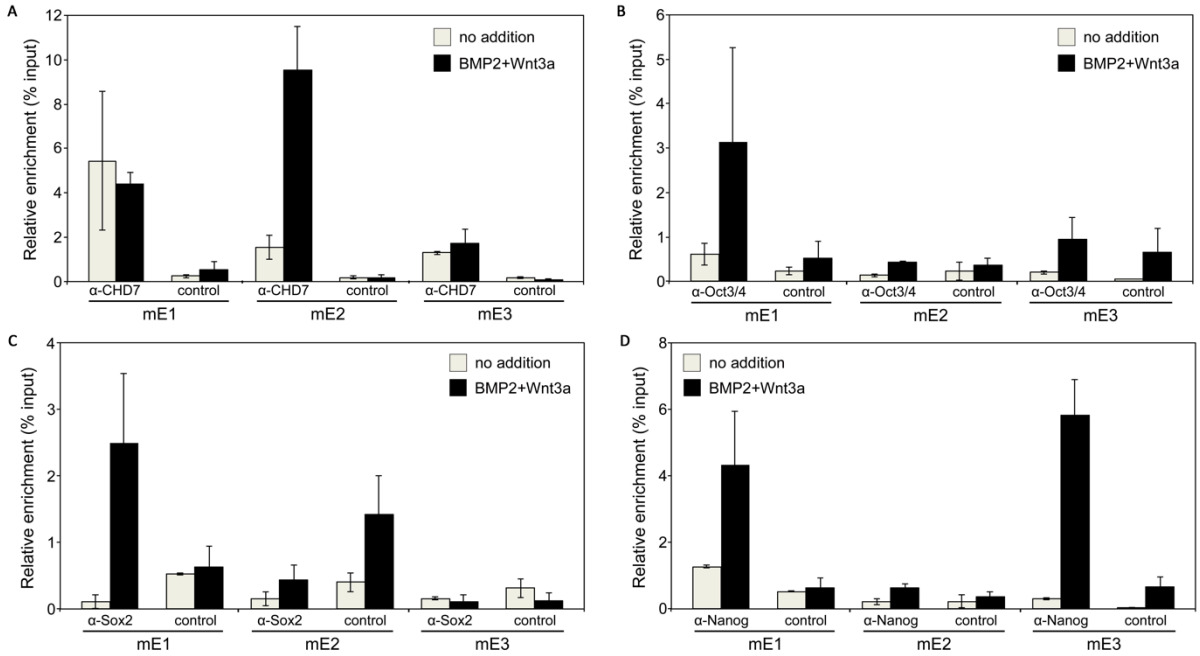

Fig. 2.5 Binding patterns of CHD7, Oct3/4, Sox2, and Nanog to the highly conserved genomic regions of mouse *FoxD3*. **(A)** μChIP-qPCR analysis using CHD7 antibodies. The *Y*-axis represents percentage of co-immunoprecipitated DNA over input. **(B)** μChIP-qPCR analysis using Oct3/4 antibodies. **(C)** μChIP-qPCR analysis using Sox2 antibodies. **(D)** μChIP-qPCR analysis using Nanog antibodies. Data are presented as mean ± SEM of 2 to 5 independent experiments.

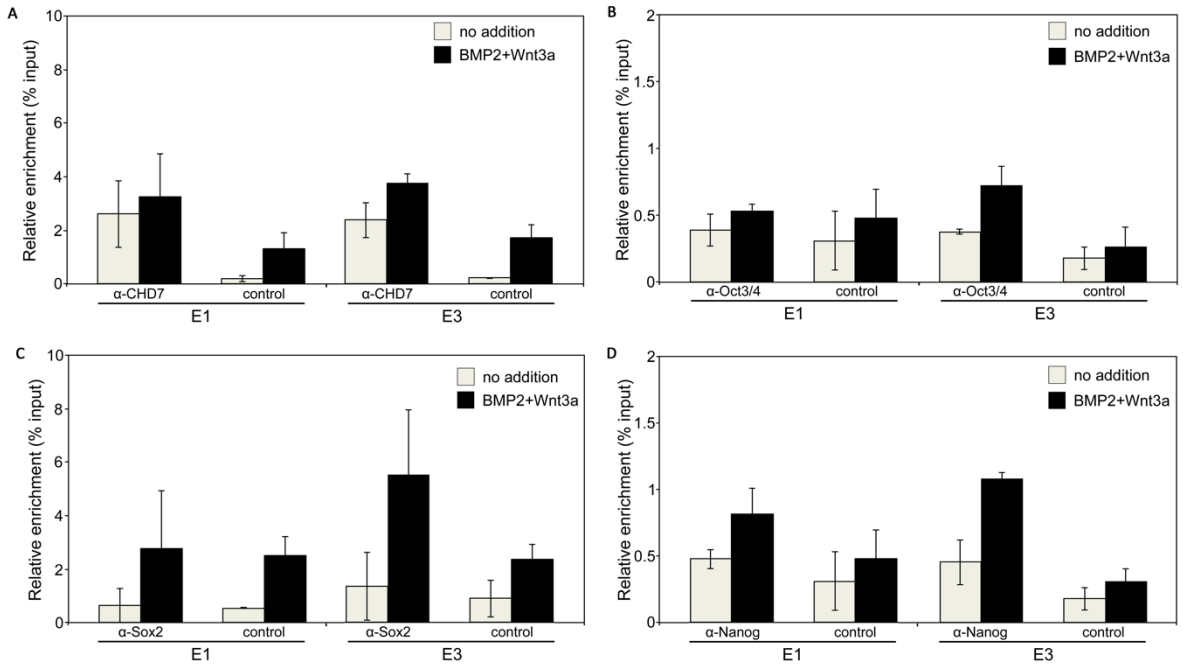

Fig. 2.6 Binding patterns of CHD7, Oct3/4, Sox2, and Nanog to the *cis*-regulatory elements of mouse *Sox9*. **(A)** μChIP-qPCR analysis using CHD7 antibodies. The *Y*-axis represents percentage of co-immunoprecipitated DNA over input. **(B)** μChIP-qPCR analysis using Oct3/4 antibodies. **(C)** μChIP-qPCR analysis using Sox2 antibodies. **(D)** μChIP-qPCR analysis using Nanog antibodies. Data are presented as mean ± SEM of 2 to 4 independent experiments.

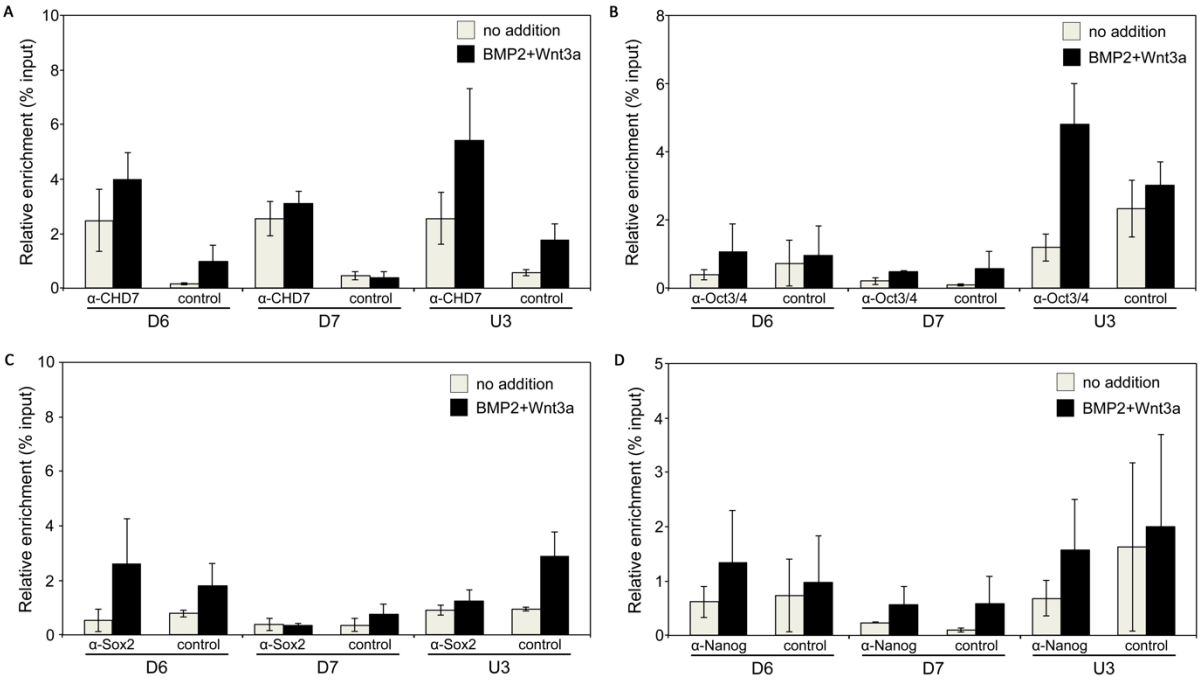

Fig. 2.7 Binding patterns of CHD7, Oct3/4, Sox2, and Nanog to the *cis*-regulatory elements of mouse *Sox10*. **(A)** μChIP-qPCR analysis using CHD7 antibodies. The *Y*-axis represents percentage of co-immunoprecipitated DNA over input. **(B)** μChIP-qPCR analysis using Oct3/4 antibodies. **(C)** μChIP-qPCR analysis using Sox2 antibodies. **(D)** μChIP-qPCR analysis using Nanog antibodies. Data are presented as mean ± SEM of 2 to 5 independent experiments.

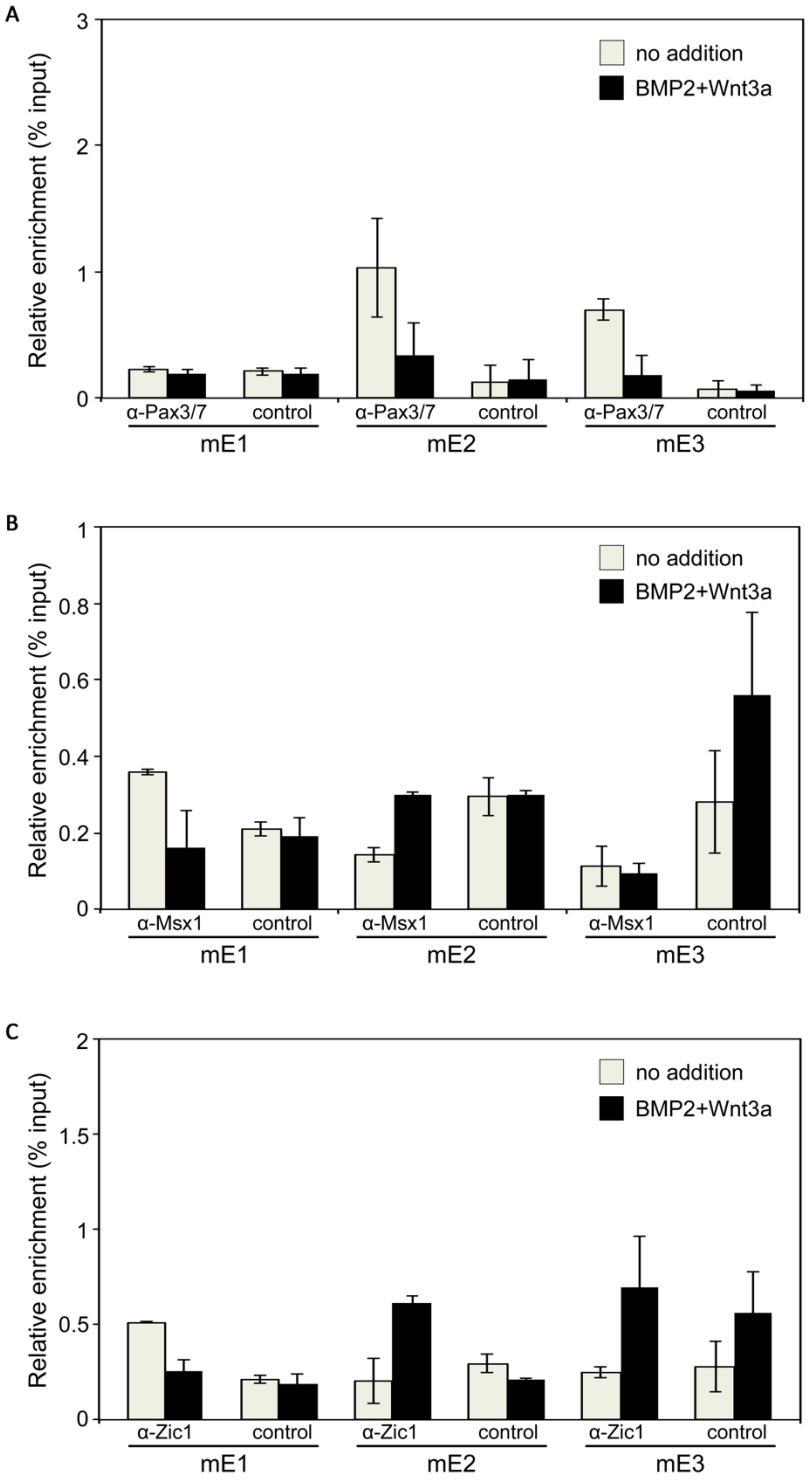

Fig. 2.8 Binding patterns of Pax3/7, Msx1, and Zic1 to the highly conserved genomic regions of mouse *FoxD3*. **(A)** μChIP-qPCR analysis using Pax3/7 antibodies. The *Y*-axis represents percentage of co-immunoprecipitated DNA over input. **(B)** μChIP-qPCR analysis using Msx1 antibodies. **(C)** μChIP-qPCR analysis using Zic1 antibodies. Data are presented as mean ± SEM of 2 to 3 independent experiments.

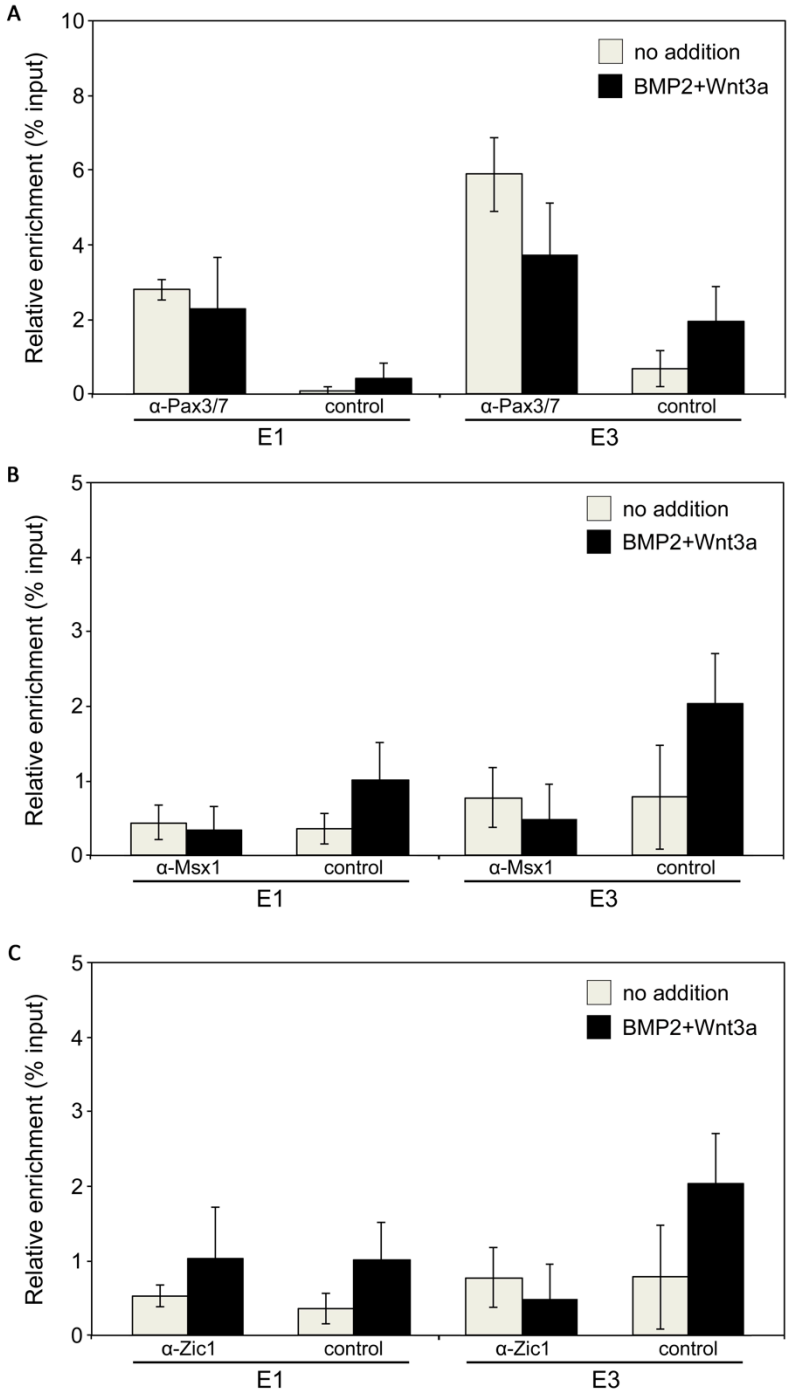

Fig. 2.9 Binding patterns of Pax3/7, Msx1, and Zic1 to the *cis*-regulatory elements of mouse *Sox9*. **(A)** μChIP-qPCR analysis using Pax3/7 antibodies. The *Y*-axis represents percentage of co-immunoprecipitated DNA over input. **(B)** μChIP-qPCR analysis using Msx1 antibodies. **(C)** μChIP-qPCR analysis using Zic1 antibodies. Data are presented as mean ± SEM of 2 to 3 independent experiments.

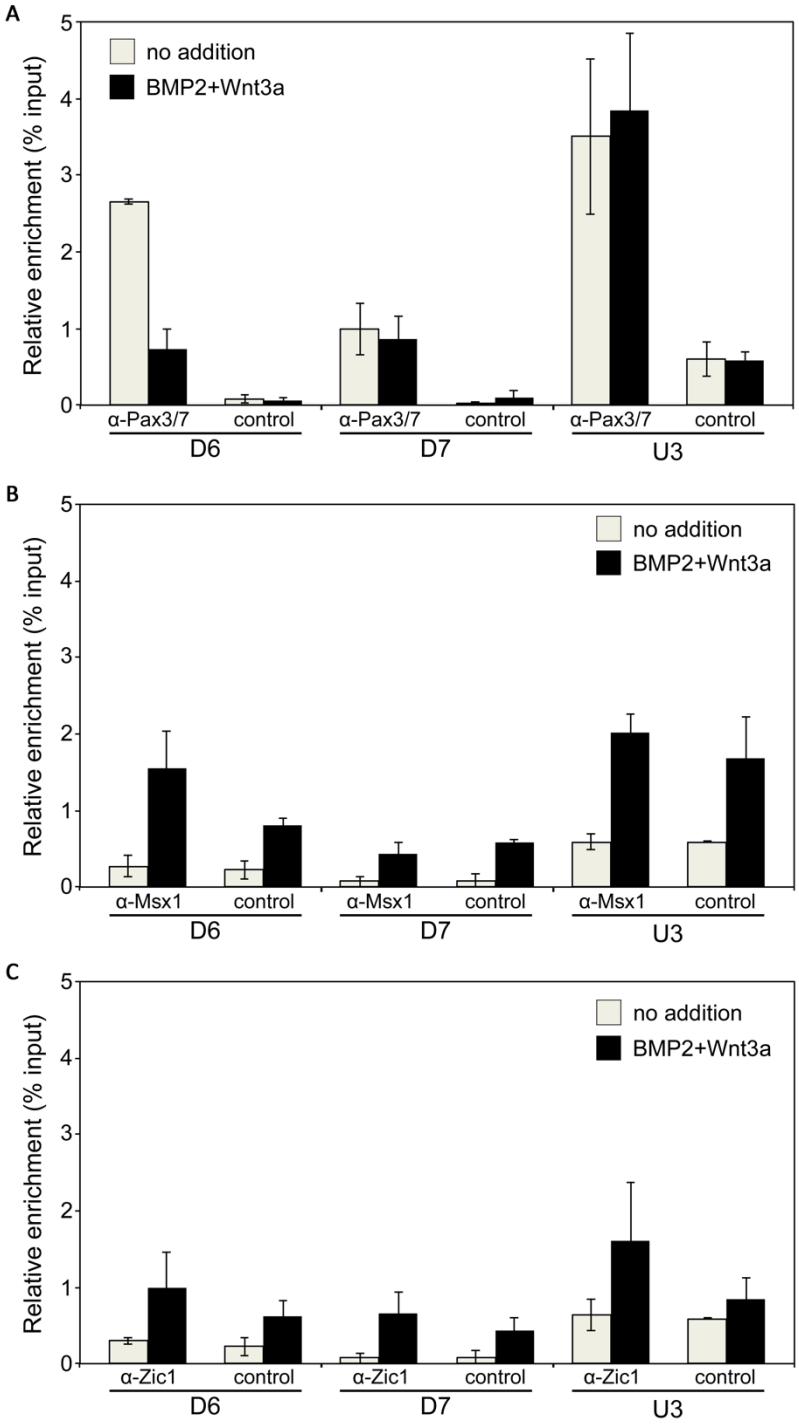

Fig. 2.10 Binding patterns of Pax3/7, Msx1, and Zic1 to the *cis*-regulatory elements of mouse *Sox10*. **(A)** μChIP-qPCR analysis using Pax3/7 antibodies. The *Y*-axis represents percentage of co-immunoprecipitated DNA over input. **(B)** μChIP-qPCR analysis using Msx1 antibodies. **(C)** μChIP-qPCR analysis using Zic1 antibodies. Data are presented as mean ± SEM of 2 to 4 independent experiments.

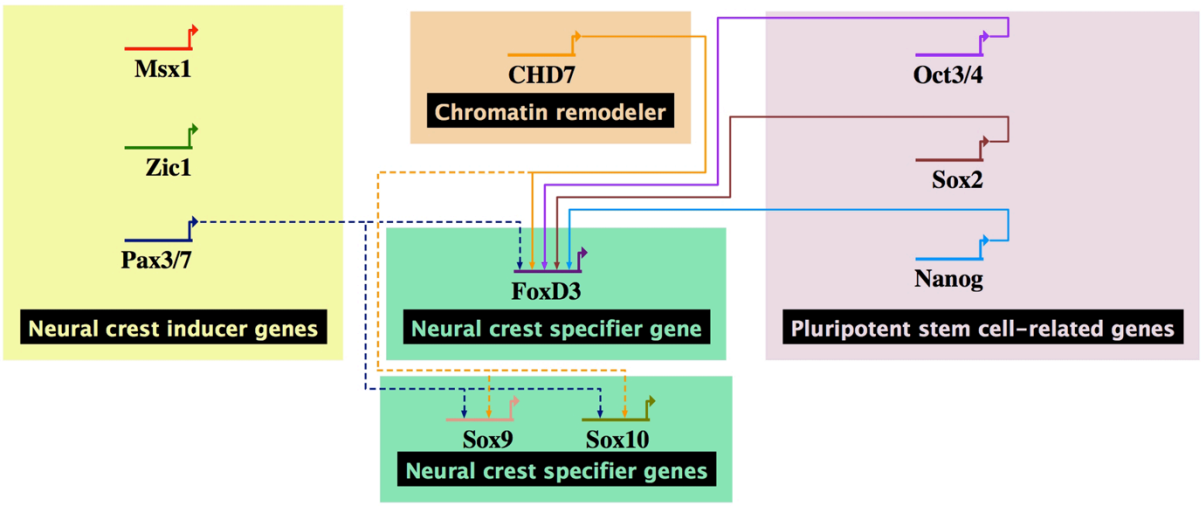

Fig. 2.11 Summary for binding patterns of CHD7, Pax3/7, Msx1, Zic1, Oct3/4, Sox2, and Nanog to the *cis*-elements of neural crest specifier genes. Solid lines indicate the direct binding in BMP2/Wnt3a-depemdent manner. Dotted lines show the BMP2/Wnt3a-independent binding.

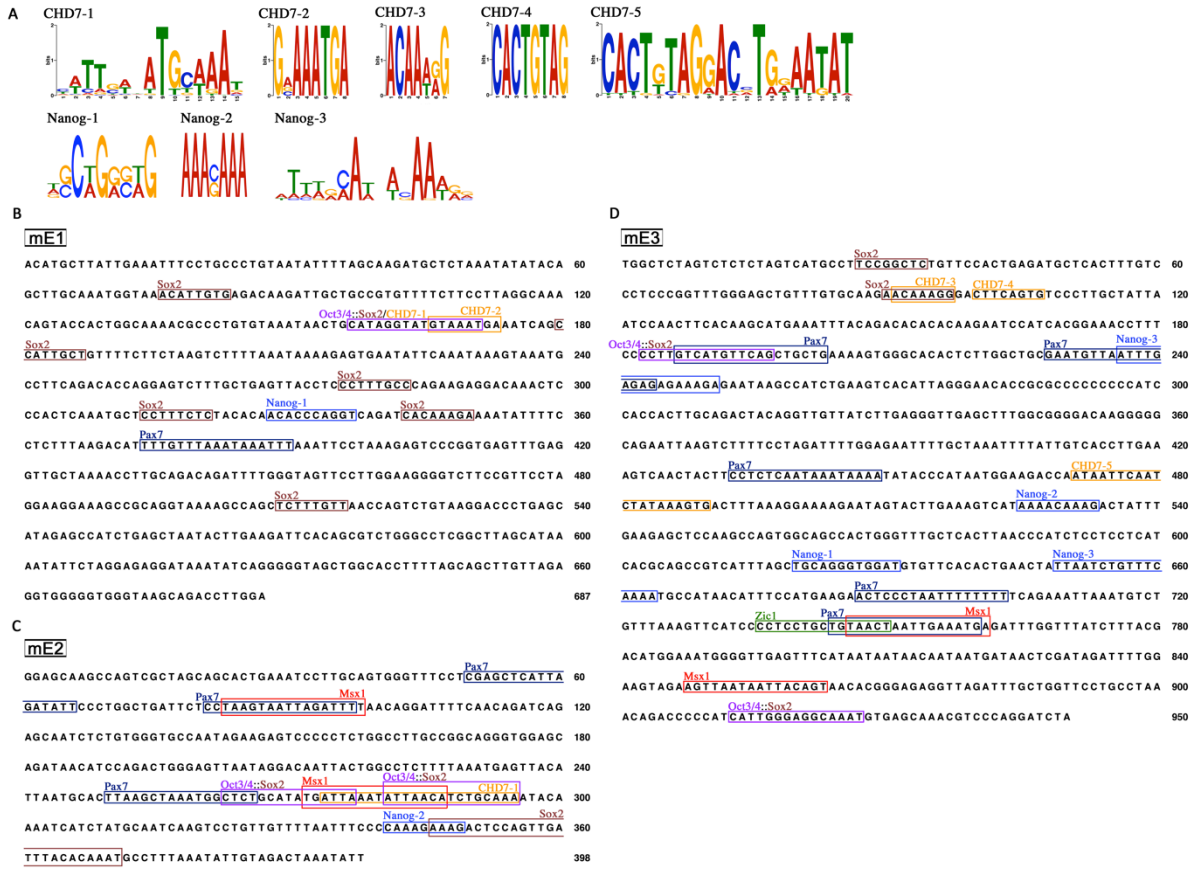

Fig. 2.12 Binding sites of CHD7, Pax3/7, Msx1, Zic1, Oct3/4, Sox2, and Nanog in the *cis*-elements of mouse *FoxD3*. **(A)** Enrichment of CHD7 and Nanog consensus DNA motifs in ChIP-seq peaks [20, 66] observed in the *cis*-elements of mouse *FoxD3*. **(B-D)** Binding sites of CHD7, the products of pluripotent stem cell-related genes, and the products of neural crest inducer genes in mE1 (B), mE2 (C), and mE3 (D) of mouse *FoxD3*.

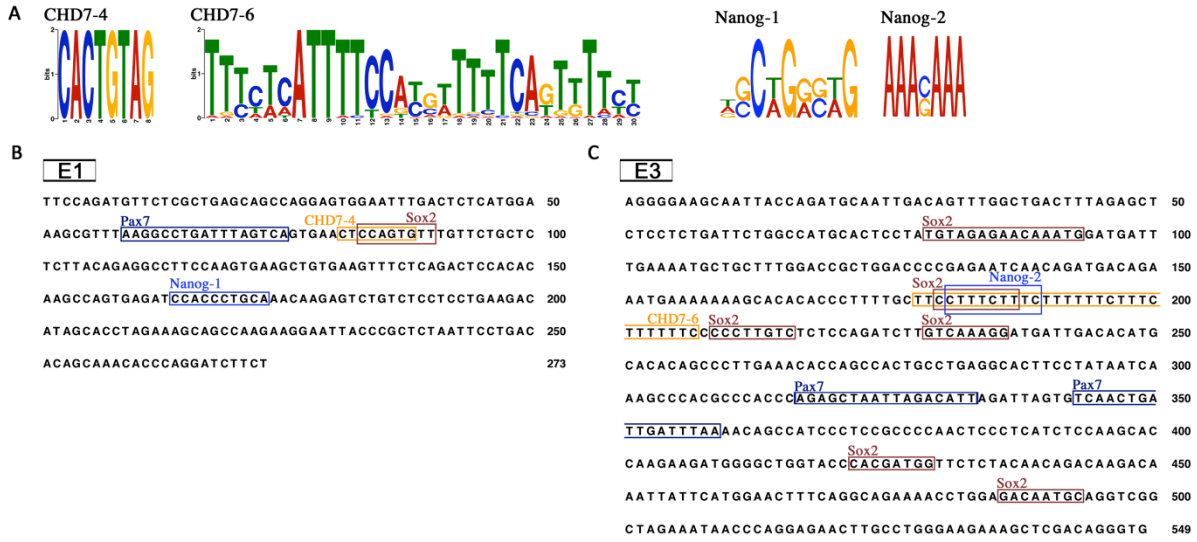

Fig. 2.13 Binding sites of CHD7, Pax3/7, Msx1, Zic1, Oct3/4, Sox2, and Nanog in the *cis*-regulatory elements of mouse *Sox9*. **(A)** Enrichment of CHD7 and Nanog consensus DNA motifs in ChIP-seq peaks [20, 66] observed in the *cis*-regulatory elements of mouse *Sox9*. **(B and C)** Binding sites of CHD7, the products of pluripotent stem cell-related genes, and the products of neural crest inducer genes in E1 (B) and E2 (C) of mouse *Sox9*.

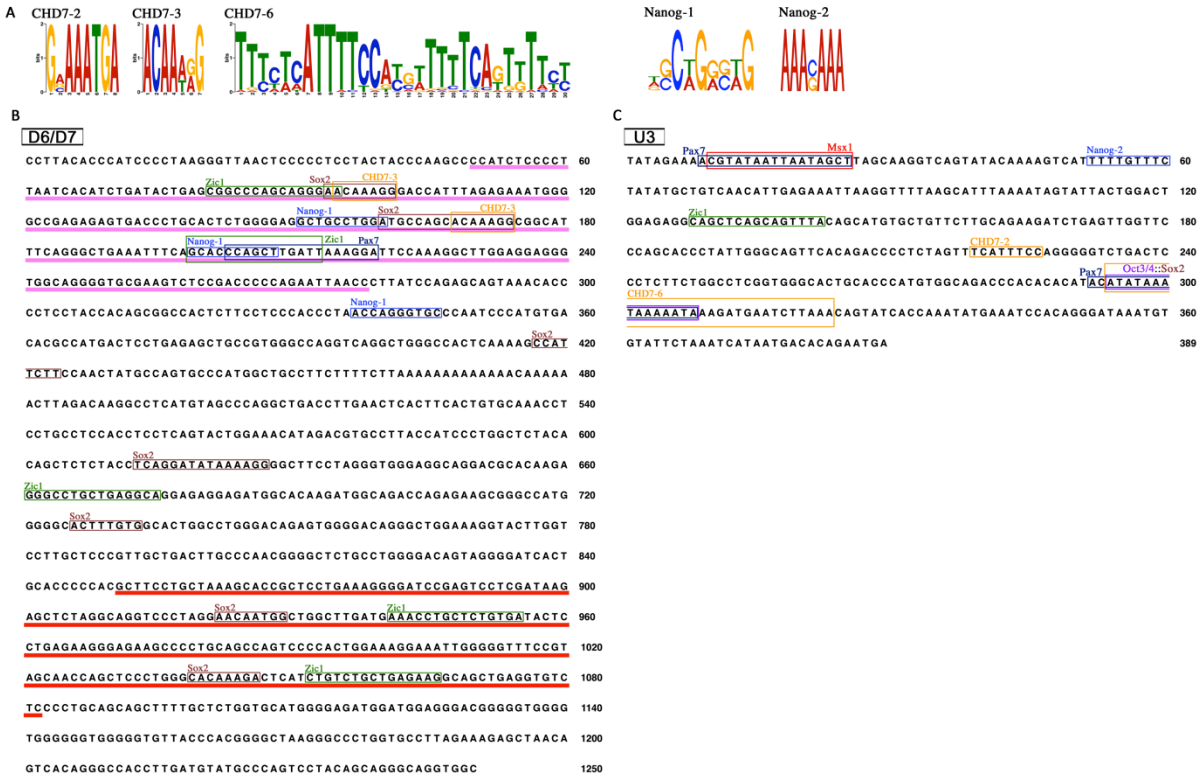

Fig. 2.14 Binding sites of CHD7, Pax3/7, Msx1, Zic1, Oct3/4, Sox2, and Nanog in the *cis*-regulatory elements of mouse *Sox10*. **(A)** Enrichment of CHD7 and Nanog consensus DNA motifs in ChIP-seq peaks [20, 66] observed in the *cis*-regulatory elements of mouse *Sox10*. **(B and C)** Binding sites of CHD7, the products of pluripotent stem cell-related genes, and the products of neural crest inducer genes in D6/D7 (B) and U3 (C) of mouse *Sox10*. The regions of D6 and D7 are shown by the pink or red underlines, respectively (B).

FoxD3 expression is suppressed by the knockdown of *CHD7*, *Oct3/4*, *Sox2*, or *Nanog*

Our present data strongly suggest that the formation of mouse NCSCs by BMP2/Wnt3a is promoted by the direct regulation of FoxD3 expression by CHD7, Oct3/4, Sox2, and Nanog. Therefore, we examined the effects of CHD7, Oct3/4, Sox2, and Nanog on FoxD3 expression in mouse trunk neural crest cell cultures. Overexpression of CHD7 or

BMP/Wnt3a treatment significantly stimulated FoxD3 and Sox10 expression (Fig. 2.15A-H). These treatments also increased the proportion of cells expressing both FoxD3 and Sox10 (Fig. 2.15I). In contrast, the expression of both FoxD3 and Sox10 was severely decreased by the knockdown of *CHD7*, *Oct3/4*, *Sox2*, or *Nanog* despite the presence of BMP2 and Wnt3a (Fig. 2.15G-H). Moreover, these siRNA treatments decreased the percentage of cells expressing both FoxD3 and Sox10 (Fig. 2.15I). These results show that the activation of *FoxD3* by CHD7, Oct3/4, Sox2, and Nanog promote Sox10 expression, leading to the formation of mouse NCSCs. This regulatory gene cascade differed from that in the neural crest induction mechanisms.

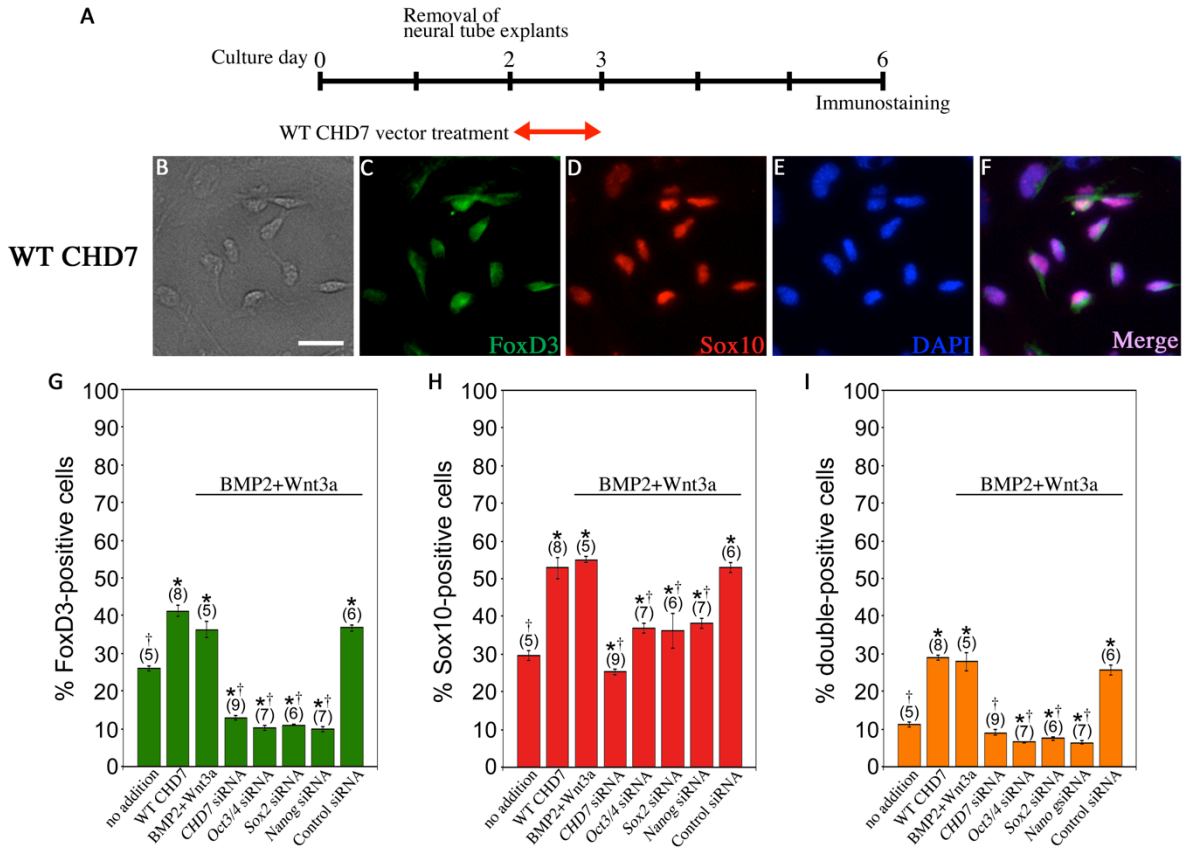

Fig. 2.15 Effects of *CHD7*, *Oct3/4*, *Sox2*, or *Nanog* siRNA on Sox10 and FoxD3 expression in mouse trunk neural crest cell cultures. **(A)** After removal of neural tube explants, the WT CHD7 expression vectors were applied from 2 days to 3 days in culture. *CHD7*, *Oct3/4*, *Sox2*, or *Nanog*

siRNA were applied from 2 days to 3 days in culture. Immunostaining with anti-Sox10 and anti-FoxD3 was performed on culture day 6. **(B)** Bright-field image in the presence of the WT CHD7 expression vectors. **(C)** Anti-FoxD3-positive cells in the same field as (B). **(D)** Anti-Sox10-positive cells in the same field as (B). **(E)** DAPI nuclear stain of the same field as (B). **(F)** Merged image of (C-E). **(G)** Percentage of cells expressing FoxD3 per total cells in a neural crest cell colony (each colony was derived from a neural tube explant). **(H)** Percentage of cells expressing Sox10 per total cells in a neural crest cell colony. **(I)** Percentage of cells expressing both Sox10 and FoxD3 per total cells in a neural crest cell colony. *, $p < 0.05$ (Student's *t*-test) compared to the untreated cultures. †, $p < 0.05$ (Student's *t*-test) compared to the BMP2/Wnt3a-treated cultures. Data are expressed as mean ± SEM of separate counts of 5-9 colonies (the number in a parenthesis on each bar). Scale Bar = 50 μm.

Histone H3K4 methylation promotes FoxD3 and Sox10 expression

Since H3K4me3 occurs in the promoter regions of transcriptionally active genes [79, 80] and CHD7 binds mainly to H3K4me1 [25], we examined the effects of H3K4 methylation on the expression of FoxD3 and Sox10. We inhibited H3K4 methylation by using siRNAs of *Setd7* (the H3K4 mono-methylation specific histone methyltransferase) [81] and of *MLL* and *Setd1a* (H3K4 tri-methylation specific histone methyltransferases) [82, 83]. These siRNA treatments suppressed FoxD3 and Sox10 expression despite the presence of BMP2/Wnt3a or CHD7 overexpression (Fig. 2.16A, C). CHD7 overexpression expectedly stimulated CHD7 expression (Fig. 2.16B). It is conceivable that Setd7, MLL, and Setd1a play important roles in the formation of mouse NCSCs. Interestingly, siRNA of *ESET*, an H3K9 tri-methylation specific histone methyltransferase

[84], inhibited Sox10 expression, although siRNA of *Suv39h1*, another H3K9 tri-methylation specific histone methyltransferase [84], had no effect on Sox10 expression (Fig. 2.16C). ESET may be involved in the formation of mouse NCSCs by repressing transcription of some differentiation-related genes.

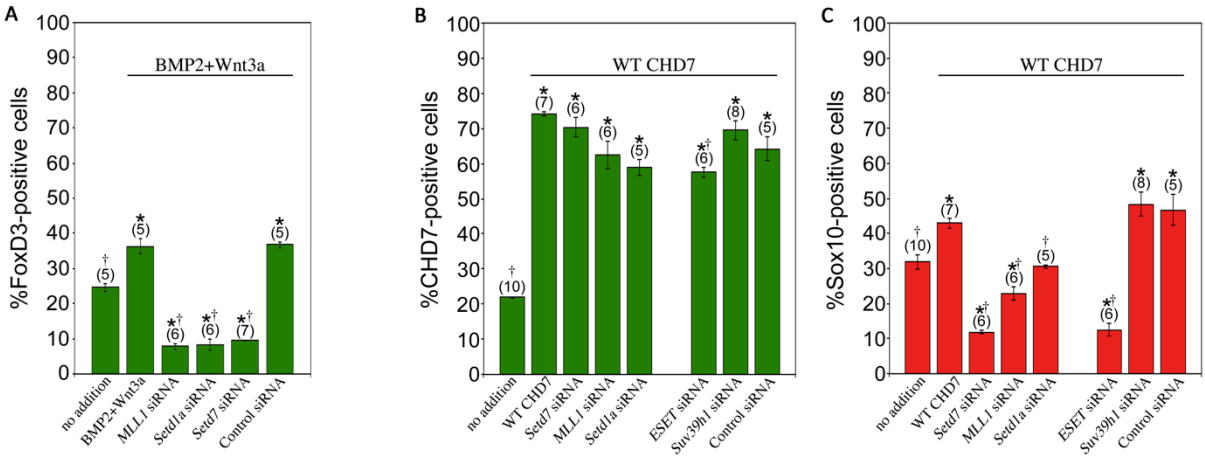

Fig. 2.16 Effects of siRNAs of histone methyltransferase genes on FoxD3, Sox10, and CHD7 expression in mouse trunk neural crest cell cultures. **(A)** Percentage of cells expressing FoxD3 per total cells in a neural crest cell colony (each colony was derived from a neural tube explant). *, $p < 0.05$ (Student's *t*-test) compared to the untreated cultures. †, $p < 0.05$ (Student's *t*-test) compared to BMP2/Wnt3a-treated cultures. Data are expressed as mean ± SEM of separate counts of 5-7 colonies (the number in a parenthesis on each bar). **(B)** Percentage of cells expressing CHD7 per total cells in a neural crest cell colony. **(C)** Percentage of cells expressing Sox10 per total cells in a neural crest cell colony. *, $p < 0.05$ (Student's *t*-test) compared to the untreated cultures. †, $p < 0.05$ (Student's *t*-test) compared to the cultures transfected with WT CHD7 expression vector. Data are expressed as mean ± SEM of separate counts of 5-10 colonies (the number in a parenthesis on each bar).

Discussion

In the present study, we showed a mechanism underlying mouse NCSC formation (Fig. 2.17). Although BMP2/Wnt3a signaling and CHD7 are implicated in neural crest induction, the regulatory gene cascade in NCSC formation mechanism was drastically different from that in the neural crest induction mechanisms. CHD7, Oct3/4, Sox2, and Nanog stimulated by BMP2/Wnt3a signaling directly induce FoxD3 expression. In turn, FoxD3 promotes the expression of Sox10, which is an indispensable transcription factor for mouse NCSC formation [9, 63]. The products of neural crest inducer genes such as *Pax3/7*, *Zic1*, and *Msx1* have been known to regulate FoxD3 expression in neural crest induction [6]. However, our μChIP-qPCR assays showed that CHD7, Oct3/4, Sox2, and Nanog stimulated by BMP2/Wnt3a signaling directly bind to *FoxD3* conserved regions in mouse NCSC formation. On the other hand, Pax3/7, Zic1, and Msx1 did not bind to the *FoxD3* conserved genomic regions in a BMP2/Wnt3a-dependent manner. The inhibition of the expression of CHD7, Oct3/4, Sox2, and Nanog suppressed FoxD3 expression. Furthermore, *FoxD3* siRNA repressed Sox10 expression. This latter result is consistent with the observation that FoxD3 binds to the U3 enhancer element of *Sox10* and activates *Sox10* [78]. Thus, these data suggest that the binding of CHD7, Oct3/4, Sox2, and Nanog to *FoxD3 cis*-regulatory elements in a BMP2/Wnt3a-dependent manner plays important roles in the formation of mouse NCSCs expressing Sox10. Schnetz et al. (2010) [25] have reported that CHD7, Oct3/4, Sox2, and Nanog colocalize at active gene enhancer elements in ES cells. Furthermore, Oct3/4, Sox2, Nanog, and FoxD3 interact with each other to maintain the pluripotency of ES cells [85]. A physical association between Oct3/4 and FoxD3 in ES cells was also reported [86]. Therefore, the mechanism underlying NCSC formation

presented in this study may be similar to that underlying the maintenance mechanism of the pluripotency of ES cells.

Sox9 siRNA suppressed Sox10 expression in the presence of BMP2/Wnt3a. Since Sox9 has been known to bind to the U3 enhancer element of *Sox10* [78], Sox9 as well as FoxD3 may control mouse NCSC formation. However, our μChIP-qPCR assays showed no enrichment of CHD7, Oct3/4, Sox2, Nanog, Pax3/7, Zic1, or Msx1 at *Sox9* enhancer elements E1 and E3 in a BMP2/Wnt3a-dependent manner. It is conceivable that other factors and/or other regulatory elements participate in Sox9 activation, leading to mouse NCSC formation.

The present data revealed that mono- and/or tri-methylation of H3K4 is necessary for the expression of Sox10 and FoxD3. It has been reported that CHD7 binds to the enhancer elements marked with H3K4me1 in neural crest induction [21]. The BMP2/Wnt3a-dependent binding of CHD7 to the mE2 regulatory region of *FoxD3* may be due to the mono-methylation of H3K4 in mE2. Since the binding of CHD7 to enhancer elements promotes gene activation [26, 27], it is conceivable that the binding of this chromatin remodeler to mE2 stimulates FoxD3 expression in mouse NCSC formation. Sox10 expression was suppressed by the inhibition of H3K4 mono-methylation despite CHD7 overexpression. As the predominant binding of CHD7 to *Sox10* regulatory regions was not observed, the inhibition of FoxD3 expression might cause this suppression. Moreover, H3K4 is tri-methylated in TSS of transcriptionally active genes [79, 87]. It is possible that the tri-methylation of H3K4 in TSS of *FoxD3* and *Sox10* activates these genes and leads to the formation of mouse NCSCs. ESET, an H3K9 tri-methylation specific histone methyltransferase, was involved in mouse NCSC formation, although Suv39h1, another H3K9 tri-methylation specific histone methyltransferase, had no effect on NCSC formation. ESET has been shown to repress the expression of trophoectoderm-associated

genes *Cdx2*, *Gata2*, and *Hand1*, and thereby to participate in the maintenance of the pluripotency of ES cells [88]. These transcriptional factors act on neural crest development [89, 90]. Furthermore, Fei et al. (2015) [91] have reported that the interaction between ESET and PRC2 maintains the pluripotency of ES cells. Thus, the downregulation of differentiation-related genes by ESET may be crucial for maintaining the multipotency of mouse neural crest cells and for the formation of mouse NCSCs.

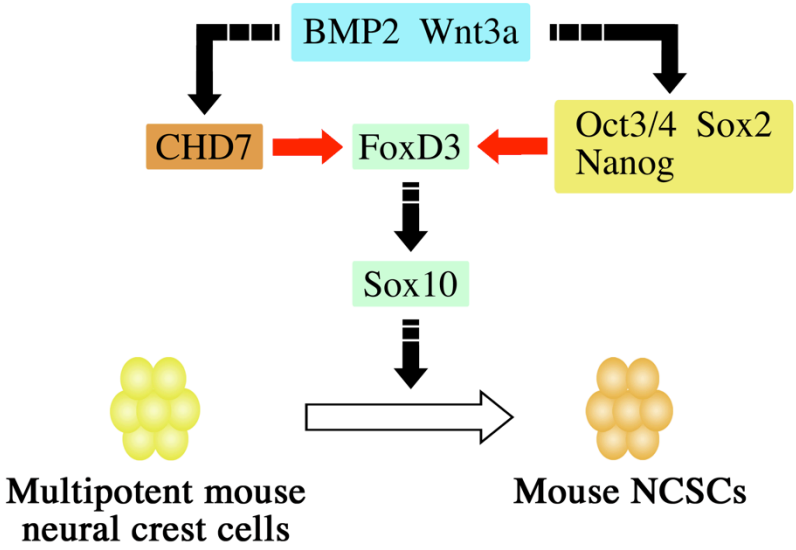

Fig. 2.17 Model for a regulatory gene cascade in the formation of mouse NCSCs. The multipotency of neural crest cells is maintained by BMP2/Wnt3a signaling. CHD7, Oct3/4, Sox2, and Nanog activated by BMP2/Wnt3a directly bind to the *FoxD3 cis*-regulatory elements and activate this gene. FoxD3 promotes Sox10 expression and leads to mouse NCSC formation.

Conclusion

1. Undifferentiated mouse trunk neural crest cells express Sox10, which is indispensable for the maintenance of the undifferentiated state of neural crest cells, and p75. We have examined the expression of CHD7, one of chromatin remodelers, in mouse trunk neural crest cells. CHD7 expression was found in the early migratory neural crest cells containing Sox10 or p75. Moreover, co-expression of CHD7 and Sox10 was observed in the dorsal neural tube containing premigratory neural crest cells. These data suggest that undifferentiated mouse trunk neural crest cells express CHD7 as well as Sox10 and p75.

2. We have examined the temporal change of CHD7 expression in mouse trunk neural crest cell cultures. The number of the undifferentiated neural crest cells expressing Sox10 or p75 decreased from culture day 2 to culture day 6. Furthermore, the expression of CHD7 was also suppressed with time.

3. The treatment of 10 ng/ml BMP2 and 10 ng/ml Wnt3a promoted the expression of CHD7, Sox10, or p75 on culture day 6. High concentration of Wnt3a (100 ng/ml) alone showed the similar effects. When BMP activities in FBS and/or CEE was prevented by noggin and chordin, these inhibitors had no effects on CHD7 or Sox10 expression in the presence of BMP2/Wnt3a or 100 ng/ml Wnt3a. These data suggest that the activation of Wnt signaling is a key requisite for the maintenance of CHD7 expression and thus for the maintenance of the undifferentiated state of neural crest cells, and that BMP signaling plays supportive roles in the maintenance of the undifferentiated state of these cells. Further, when we used BIO instead of Wnt3a, BIO treatment promoted the expression of CHD7 and/or Sox10. The addition of the DN β-catenin or the DN TCF expression vectors in the

presence of BMP2 and Wnt3a significantly suppressed the expression of CHD7 and/or Sox10. Thus, Wnt/β-catenin pathway may play important roles in the maintenance of the undifferentiated state of mouse trunk neural crest cells.

4. The addition of WT CHD7 expression vectors significantly promoted the expression of Sox10 or p75 and the co-expression of CHD7/Sox10 or CHD7/p75. On the other hand, cells expressing CHD7, Sox10, and/or p75 were significantly suppressed by the treatment of DN CHD7 expression vectors or *CHD7* siRNA in the presence of BMP2 and Wnt3a. These results show that CHD7 is required for the maintenance of the undifferentiated state of mouse trunk neural crest cells.

5. Since undifferentiated neural crest cells may be multipotential, CHD7 and BMP2/Wnt3a may participate in maintaining the multipotency of mouse trunk neural crest cells. It has been known that multipotent trunk neural crest cells can differentiate into smooth muscle cells, neurons, and glia. Therefore, we investigated whether or not the activation of CHD7 or BMP2/Wnt3a signaling increases the number of multipotent mouse trunk neural crest cells that differentiate into smooth muscle cells, neurons, and glia. The addition of WT CHD7 expression vectors or BMP2/Wnt3a significantly increased the proportion of clones consisting of both smooth muscle cells and neurons or both smooth muscle cells and glia. These data suggest that BMP2/Wnt3a signaling and CHD7 plays essential roles in the maintenance of the multipotency of mouse trunk neural crest cells. Moreover, adult mouse DRG and sciatic nerves contained Sox10- and/or p75-positive NCSCs expressing CHD7. These results suggest that CHD7 as well as Sox10 participates in the maintenance of the multipotency of neural crest cells and conduct them to mouse NCSCs expressing p75.

6. BMP2/Wnt3a signaling and CHD7 maintain the multipotency of mouse trunk neural crest cells and lead to the formation of mouse NCSCs. Since it has been shown that these factors activate neural crest specifier genes, such as *Sox9*, *Sox10*, *FoxD3*, in neural crest induction, we examined roles of these genes in the formation of mouse NCSCs. Knockdown of *Sox9* or *FoxD3* significantly suppressed Sox10 expression even under BMP2/Wnt3a-treated conditions. Data indicate that FoxD3 and Sox9 promote Sox10 expression in the formation of mouse NCSCs.

7. It has been known that the products of neural crest inducer genes, such as *Pax3/7*, *Zic1*, and *Msx1*, activate *FoxD3* and *Sox9* in neural crest development. Moreover, CHD7 has been known to interact with the pluripotent stem cell-related genes, such as *Oct3/4*, *Sox2*, and *Nanog*, in ES cells. Therefore, we examined the binding of neural crest inducer genes and pluripotent stem cell-related genes to the *cis*-elements of *Sox9*, *Sox10*, and *FoxD3* by μChIP-qPCR assays. CHD7, Oct3/4, Sox2, and Nanog bound to the *FoxD3 cis*-elements only in a BMP2/Wnt3a-dependent manner. In addition, we defined putative binding sites of CHD7, Oct3/4, Sox2 and Nanog within *FoxD3 cis*-elements. These results suggest that CHD7, Oct3/4, Sox2, and Nanog bind directly to the *FoxD3 cis*-elements in mouse NCSC formation.

8. Since BMP2/Wnt3a-dependent direct binding of CHD7, Oct3/4, Sox2 and Nanog to *FoxD3 cis*-elements may be essential for the formation of mouse NCSCs, we examined the effects of CHD7, Oct3/4, Sox2, and Nanog on FoxD3 expression in mouse trunk neural crest cell cultures. The addition of WT CHD7 expression vectors or BMP2/Wnt3a treatments significantly increased the number of cells expressing FoxD3 and/or Sox10. On the other hand, knockdown of *CHD7*, *Oct3/4*, *Sox2*, or *Nanog* drastically decreased the number of cells

expressing FoxD3 and/or Sox10 despite the presence of BMP2/Wnt3a. These data suggest that the activation of *FoxD3* by CHD7, Oct3/4, Sox2, and Nanog promoted the Sox10 expression, leading to the formation of mouse NCSCs. This regulatory gene cascade was dramatically different from that in the mechanisms of neural crest induction.

9. Since CHD7 binds mainly to H3K4me1 regions in *cis*-elements of target genes and H3K4me3 occurs in the promoter regions of transcriptionally active genes, we examined the effects of H3K4 methylation on the expression of FoxD3 and Sox10. Treatments with siRNAs of *Setd7* (the H3K4 mono-methylation specific histone methyltransferase), *MLL1*, and *Setd1a* (H3K4 tri-methylation specific histone methyltransferases) significantly suppressed FoxD3 and Sox10 expression despite the presence of BMP2/Wnt3a or overexpression of CHD7. These data show that Setd7, MLL, and Setd1a play important roles in the formation of mouse NCSCs. siRNA of *ESET*, a H3K9 tri-methylation specific histone methyltransferase, inhibited Sox10 expression. ESET may be implicated in the formation of mouse NCSCs by repressing transcription of some differentiation-related genes.

Acknowledgements

I would like to thank Dr. Kazuo Ito for his great advices and supports. I would like to thank Drs. Jane B. Trepel for providing pcDNA3 encoding the human DN TCF and pcDNA4 encoding the mouse DN β-catenin, Joanna Wysocka for providing pcDNA3.1 encoding the human WT CHD7 and pcDNA3.1 encoding the human DN CHD7. I would also like to thank Dr. Takuro Nakagawa for advice and help in ChIP assays and Ms. Noriko Takashima and Ms. Yasue Okada for assistance to my student life. These works were partly supported by JSPS KAKENHI Grant Number 13J01417 and Research Grant from Foundation Tokyo Institute of Technology (27KEN-075) to K., F. Finally, I thank all members of laboratory of Interdisciplinary Biology, my family and my friends for their encouragement.

References

1 Hall, B.K., 1999. The Neural Crest in Development and Evolution. Springer, New York.

2 Le Douarin, N.M., Kalcheim, C., 1999. The Neural Crest, second ed. Cambridge University Press, Cambridge.

3 Knecht, A.K., Brooner-Fraser, M., 2002. INDUCTION OF THE NEURAL CREST: A MULTIGENE PROCESS. Nat. Rev. Genet. 3, 453-461.

4 Steventon, B., Araya, C., Linker, C., Kuriyama, S., Mayor, R. 2009. Differential requirements of BMP and Wnt signalling during gastrulation and neurulation define two steps in neural crest induction. Development 136, 771-779.

5 Stuhlmiller, T.J., García-Castro, M.I., 2012. Current perspectives of the signaling pathways directing neural crest induction. Cell. Mol. Life Sci. 69, 3715-3737.

6 Sauka-Spengler, T., Bronner-Fraser, M., 2008. A gene regulatory network orchestrates neural crest formation. Nat. Rev. Mol. Cell Biol. 9, 557-568.

7 Plouhinec, J.L., Roche, D.D., Pegoraro, C., Figueiredo, A.L., Maczkowiak, F., Brunet, L.J., Milet, C., Vert, J.P., Pollet, N., Harland, R.M., Monsoro-Burq, A.H., 2014. Pax3 and Zic1 trigger the early neural crest gene regulatory network by the direct activation of multiple key neural crest specifiers. Dev. Biol. 386, 461-472.

8 Prasad, M.S., Sauka-Spengler, T., LaBonne, C., 2012. Induction of the neural crest state: control of stem cell attributes by gene regulatory, post-transcriptional and epigenetic interactions. Dev. Biol. 366, 10-21.

9 Kim, J., Lo, L., Dormand, E., Anderson, D.J., 2003. SOX10 maintains multipotency and inhibits neuronal differentiation of neural crest stem cells. Neuron 38, 17-31.

10 Nagoshi, N., Shibata, S., Nakamura, M., Matsuzaki, Y., Toyama, Y., Okano, H., 2009. Neural Crest-Derived Stem Cells Display a Wide Variety of Characteristics. J. Cell Biochem. 107, 1046-1052.

11 Shakhova, O., Sommer, L., 2010. Neural crest-derived stem cells. StemBook. 1-20.

12 Achilleos, A., Trainor, P.A., 2012. Neural crest stem cells: discovery, properties and potential for therapy. Cell Res. 22, 288-304.

13 Sieber-Blum, M., 2012. NEURAL CREST STEM CELLS. World Scientific. Singapore.

14 Li, H.Y., Say, E.H.M., Zhou, X.F., 2007. Isolation and Characterization of Neural Crest Progenitors from Adult Dorsal Root Ganglia. Stem Cells 25, 2053-2065.

15 Nagoshi, N., Shibata, S., Kubota, Y., Nakamura, M., Nagai, Y., Satoh, E., Morikawa, S., Okada, Y., Mabuchi, Y., Katoh, H., Okada, S., Fukuda, K., Suda, T., Matsuzaki, Y., Toyama, Y., Okano, H., 2008. Ontogeny and Multipotency of Neural Crest-Derived Stem Cells in Mouse Bone Marrow, Dorsal Root Ganglia, and Whisker Pad. Cell Stem Cell 2, 392-403.

16 Morrison, S.J., White, P.M., Zock, C., Anderson, D.J., 1999. Prospective Identification, Isolation by Flow Cytometry, and In Vivo Self-Renewal of Multipotent Mammalian Neural Crest Stem Cells. Cell 96, 737-749.

17 Joseph, N.M., Mukouyama, Y., Mosher, J.T., Jaegle, M., Crone, S.A., Dormand, E.L., Lee, K.F., Meijer, D., Anderson, D.J., Morrison1, S.J., 2004. Neural crest stem cells undergo multilineage differentiation in developing peripheral nerves to generate endoneurial fibroblasts in addition to Schwann cells. Development 131, 5599-5612.

18 Kruger, G.M., Mosher, J.T., Bixby, S., Joseph, N., Iwashita, T., Morrison, S.J., 2002. Neural Crest Stem Cells Persist in the Adult Gut but Undergo Changes in Self-Renewal, Neuronal Subtype Potential, and Factor Responsiveness. Neuron 35, 657-669.

19 Bixby, S., Kruger, G.M., Mosher, J.T., Joseph, N.M., Morrison, S.J., 2004. Cell-Intrinsic Differences between Stem Cells from Different Regions of the Peripheral Nervous System Regulate the Generation of Neural Diversity. Neuron 35, 643-656.

20 Rao, M.S., Anderson, D.J., 1997. Immortalization and controlled in vitro differentiation of murine multipotent neural crest stem cells. J. Neurobiol. 32, 722-746.

21 Bajpai, R., Chen, D.A., Rade-lglesias, A., Zhang, J., Xiong, Y., Helms, J., Chang, C.P., Zhao, Y., Swigut, T., Wysocka, J., 2010. CHD7 cooperates with PBAF to control multipotent neural crest formation. Nature 463, 958-964.

22 Zentner, G.E., Layman, W.S., Martin, D.M., Scacheri, P.C., 2010. Molecular phenotypic aspects of *CHD7* mutation in CHARGE syndrome. Am. J. Med. Genet. A. 152A, 674-686.

23 Siebert, J.R., Graham, J.M. Jr., MacDonald, C., 1985. Pathologic features of the CHARGE association: support for involvement of the neural crest. Teratology 31, 331-336.

24 Patten, S.A., Jacobs-McDaniels, N.L., Zaouter, C., Drapeau, P., Albertson, R.C., Moldovan, F., 2012. Role of Chd7 in Zebrafish: A Model for CHARGE Syndrome. PLoS ONE 7, e31650.

25 Schnetz, M.P., Handoko, L., Akhtar-Zaidi, B., Bartels, C.F., Pereira, C.F., Fisher, A.G., Adams, D.J., Flicek, P., Crawford, G.E., LaFramboise, T., Tesar, P., Wei, C.L., Scacheri, C., 2010. CHD7 Targets Active Gene Enhancer Elements to Modulate ES Cell-Specific Gene Expression. PLoS Gent. 6, e1001023.

26 Liu, Y., Harmelink, C., Peng, Y., Chen, Y., Wang, Q., Jiao, K., 2014. CHD7 interacts with BMP R-SMADs to epigenetically regulate cardiogenesis in mice. Hum. Mol. Genet. 23, 2145-2156.

27 Engelen, E., Akinci, U., Bryne, J.C., Hou, J., Gontan, C., Moen, M., Szumska, D., Kockx, C., van Ijcken, W., Dekkers, D.H., Demmers, J., Rijkers, E.J., Bhattacharya, S., Philipsen, S., Pevny, L.H., Grosveld, F.G., Rottier, R.J., Lenhard, B., Poot, R.A., 2011. Sox2 cooperates with Chd7 to regulate genes that are mutated in human syndromes. Nat. Genet. 43, 607-611.

28 Jones, K.M., Sarić, N., Russell, J.P., Andoniadou, C.L., Scambler, P.J., Basson, M.A., 2015. CHD7 maintains neural stem cell quiescence and prevents premature stem cell depletion in the adult hippocampus. Stem Cells 33, 196-210

29 Tomita, Y., Matsumura, K., Wakamatsu, Y., Matsuzaki, Y., Shibuya, I., Kawaguchi, H., Ieda, M., Kanakubo, S., Shimazaki, T., Ogawa, S., Osumi, N., Okano, H., Fukuda, K., 2005. Cardiac neural crest cells contribute to the dormant multipotent stem cell in the mammalian heart. J. Cell Biol. 170, 1135-1146.

30 Sieber-Blum, M., Grim, M., Hu, Y.F., Szeder, V., 2004. Pluripotent Neural Crest Stem Cells in the Adult Hair Follicle. Dev. Dyn. 231, 258-269.

31 Kléber, M., Lee, H.Y., Wurdak, H., Buchstaller, J., Riccomagno, M.M., Ittner, L.M., Suter, U., Epstein, D.J., Sommer, L., 2005. Neural crest stem cell maintenance by combinatorial Wnt and BMP signaling. J. Cell Biol. 169, 309-320.

32 Green, S.A., Simoes-Costa M., Bronner M.E., 2015. Evolution of vertebrates as viewed from the crest. Nature 520, 474-482.

33 Ito, K., Morita, T., Sieber-Blum, M., 1993. In vitro clonal analysis of mouse neural crest development. Dev. Biol. 157, 517-525.

34 Ito, K., Morita, T., 1995. Role of retinoic acid in mouse neural crest cell development in vitro. Dev. Dyn. 204, 211-218.

35 Ishikawa, S., Ito, K., 2009. Plasticity and regulatory mechanisms of Hox gene expression in mouse neural crest cells. Cell Tissue Res. 337, 381-391.

36 Ijuin, K., Nakanishi, K., Ito, K., 2008. Different downstream pathways for Notch signaling are required for gliogenic and chondrogenic specification of mouse mesencephalic neural crest cells. Mech. Dev. 125, 462-474.

37 Tetsu, O., McCormick, F., 1999. β-Catenin regulates expression of cyclin D1 in colon carcinoma cells. Nature 398, 422-426.

38 Chung, E.J., Hwang, S.G., Nguyen, P., Lee, S., Kim, J.S., Kim, J.W., Henkart, P.A., Bottaro. D.P., Soon, L., Bonvini, P., Lee, S.J., Karp, J.E., Oh, H.J., Rubin, J.S., Trepel, J.B., 2002. Regulation of leukemic cell adhesion, proliferation, and survival by β-catenin. Blood 100, 982-990.

39 Sugiura, K., Ito, K., 2010. Roles of Ets-1 and p70S6 kinase in chondrogenic and gliogenic specification of mouse mesencephalic neural crest cells. Mech. Dev. 127, 169-182.

40 Fujita, K., Yasui, S., Shinohara, T., Ito, K., 2011. Interaction between NF-κB signaling and Notch signaling in gliogenesis of mouse mesencephalic neural crest cells. Mech. Dev. 128, 496-509.

41 Hollyday, M., McMahon, J.A., McMahon, A.P., 1995. Wnt expression patterns in chick embryo nervous system. Mech. Dev. 52, 9-25.

42 Abzhanov, A., Tzahor, E., Lassar, A.B., Tabin C.J., 2003. Dissimilar regulation of cell differentiation in mesencephalic (cranial) and sacral (trunk) neural crest cells in vitro. Development 130, 4567-4579.

43 Meijer, L., Skaltsounis, A.L., Magiatis, P., Polychronopoulos, P., Knockaert, M., Leost, M., Ryan, X.P., Vonica, C.A., Brivanlou, A., Dajani, R., Crovace, C., Tarricone, C., Musacchio, A., Roe, S.M., Pearl, L., Greengard, P., 2003. GSK-3-selective inhibitors derived from Tyrian purple indirubins. Chem. Biol. 10, 1255-1266.

44 Ota, M., Ito, K., 2006. BMP and FGF-2 regulate neurogenin-2 expression and the differentiation of sensory neurons and glia. Dev. Dyn. 235:646-655.

45 Bronner-Fraser M., 2004. Development. Making sense of the sensory lineage. Science 303. 966-968.

46 Lee, H.Y., Kléber, M., Hari, L., Brault, V., Suter, U., Taketo, M.M., Kemler, R., Sommer, L., 2004. Instructive role of Wnt/beta-catenin in sensory fate specification in neural crest stem cells. Science 303, 1020-1023.

47 Mundell, N.A., Labosky, P.A., 2011. Neural crest stem cell multipotency requires Foxd3 to maintain neural potential and repress mesenchymal fates. Development 138, 641-652.

48 Vissers, L.E., van Ravenswaaij, C.M., Admiraal, R., Hurst, J.A., de Vries, B.B., Janssen, I.M., van der Vliet, W.A., Huys, E.H., de Jong, P.J., Hamel, B.C., Schoenmakers, E.F.,

Brunner, H.G., Veltman, J.A., van Kessel, A.G., 2004. Mutations in a new member of the chromodomain gene family cause CHARGE syndrome. Nature Genet. 36, 955-957.

49 Martin, D.M., 2010. Chromatin remodeling in development and disease: focus on CHD7. PLoS Genet. 6, e1001010.

50 Müller, C., Leutz, A., 2001. Chromatin remodeling in development and differentiation. Curr. Opin. Genet. Dev. 11, 167-174.

51 Sato, N., Meijer, L., Skaltsounis, L., Greengard, P., Brivanlou, A.H., 2004. Maintenance of pluripotency in human and mouse embryonic stem cells through activation of Wnt signaling by a pharmacological GSK-3-specific inhibitor. Nat. Med. 10, 55-63.

52 Sokol, S.Y., 2011. Maintaining embryonic stem cell pluripotency with Wnt signaling. Development 138, 4341-4350.

53 Tanaka, S.S., Kojima, Y., Yamaguchi, Y.L., Nishinakamura, R., Tam, P.P.L., 2011. Impact of WNT signaling on tissue lineage differentiation in the early mouse embryo. Dev. Growth Differ. 53, 843-856.

54 García-Castro, M.I., Marcelle, C., Bronner-Fraser, M., 2002. Ectodermal Wnt function as a neural crest inducer. Science 297, 848-851.

55 Ikeya, M., Lee, S.M., Johnson, J.E., McMahon, A.P., Takada, S., 1997. Wnt signalling required for expansion of neural crest and CNS progenitors. Nature 389, 966-970.

56 Hari, L., Brault, V., Kléber, M., Lee, H.Y., Ille, F., Leimeroth, R., Paratore, C., Suter, U., Kemler, R., Sommer, L., 2002. Lineage-specific requirements of beta-catenin in neural crest development. J. Cell Biol. 159, 867-880.

57 Schmidt, C., Patel, K., 2005. Wnts and the neural crest. Anat. Embryol. 209, 349-355.

58 Correia, A.C., Costa, M., Moraes, F., Bom, J., Nóvoa, A., Mallo, M., 2007. *Bmp2* is required for migration but not for induction of neural crest cells in the mouse. Dev. Dyn. 236, 2493-2501.

59 Haldin, C.E., LaBonne, C., 2010. SoxE factors as multifunctional neural crest regulatory factors. Int. J. Biochem. Cell Biol. 42, 441-444.

60 Teng, L., Mundell, N.A., Frist, A.Y., Wang, Q., Labosky, P.A., 2008. Requirement for Foxd3 in the maintenance of neural crest progenitors. Development 135, 1615-1624.

61 Hanna, L.A., Foreman, R.K., Tarasenko, I.A., Kessler, D.S., Labosky, P.A., 2002. Requirement for Foxd3 in maintaining pluripotent cells of the early mouse embryo. Genes Dev. 16, 2650-2661.

62 Plank, J.L., Suflita, M.T., Galindo, C.L., Galindo, C.L., Labosky, P.A., 2014. Transcriptional targets of Foxd3 in murine ES cells. Stem Cell Res. 12, 233-240.

63 Fujita, K., Ogawa, R., Kawawaki, S. Ito, K., 2014. Roles of chromatin remodelers in maintenance mechanisms of multipotency of mouse trunk neural crest cells in the formation

of neural crest-derived stem cells. Mech. Dev. 133, 126-145.

64 Schnetz, M.P., Bartels, C.F., Shastri, K., Balasubramanian, D., Zentner, G.E., Balaji, R., Zhang, X., Song, L., Wang, Z., Laframboise, T., Crawford, G.E., Scacheri, P.C., 2009. Genomic distribution of CHD7 on chromatin tracks H3K4 methylation patterns. Genome Res. 19, 590-601.

65 Murawska, M., Brehm, A., 2011. CHD chromatin remodelers and the transcription cycle. Transcription 2, 244-253.

66 Kikuchi, M., Hayashi, R., Kanakubo, S., Ogasawara, A., Yamato, M., Osumi, N., Nishida, K., 2011. Neural crest-derived multipotent cells in the adult mouse iris stroma. Genes Cells 16, 273-281.

67 Hagiwara, K., Obayashi, T., Sakayori, N., Yamanishi, E., Hayashi, R., Osumi, N., Nakazawa, T., Nishida, K., 2014. Molecular and cellular features of murine craniofacial and trunk neural crest cells as stem cell-like cells. PLoS One 9, e84072.

68 Dahl, J.A., Collas, P., 2008. A rapid micro chromatin immunoprecipitation assay (microChIP). Nat. Protoc. 3, 1032-1045.

69 Marson, A., Levine, S.S., Cole, M.F., Frampton, G.M., Brambrink, T., Johnstone, S., Guenther, M.G., Johnston, W.K., Wernig, M., Newman, J., Calabrese, J.M., Dennis, L.M., Volkert, T.L., Gupta, S., Love, J., Hannett, N., Sharp, P.A., Bartel, D.P., Jaenisch, R., Young, R.A., 2008. Connecting microRNA genes to the core transcriptional regulatory

circuitry of embryonic stem cells. Cell. 134, 521-533.

70 Whyte, W.A., Orlando, D.A., Hnisz, D., Abraham, B.J., Lin, C.Y., Kagey, M.H., Rahl, P.B., Lee, T.I., Young, R.A., 2013. Master transcription factors and mediator establish super-enhancers at key cell identity genes. Cell 153, 307-319.

71 Oki, S., Maehara, K., Ohkawa, Y., Meno, C., 2014. SraTailor: graphical user interface software for processing and visualizing ChIP-seq data. Genes Cells 19, 919-926.

72 Simões-Costa, MS., McKeown, S.J., Tan-Cabugao, J., Sauka-Spengler, T., Bronner, M.E., 2012. Dynamic and differential regulation of stem cell factor FoxD3 in the neural crest is Encrypted in the genome. PLoS Genet. 8, e1003142.

73 Machanick, P., Bailey, T.L., 2011. MEME-ChIP: motif analysis of large DNA datasets. Bioinformatics 27, 1696-1697.

74 Loh, Y.H., Wu, Q., Chew, J.L., Vega, V.B., Zhang, W., Chen, X., Bourque, G., George, J., Leong, B., Liu, J., Wong, K.Y., Sung, K.W., Lee, C.W., Zhao, X.D., Chiu, K.P., Lipovich, L., Kuznetsov, V.A., Robson, P., Stanton, L.W., Wei, C.L., Ruan, Y., Lim, B., Ng, H.H., 2006. The Oct4 and Nanog transcription network regulates pluripotency in mouse embryonic stem cells. Nat. Genet. 38, 431-440.

75 Pan, G., Thomson, J.A., 2007. Nanog and transcriptional networks in embryonic stem cell pluripotency. Cell Res. 17, 42-49.

76 Bagheri-Fam, S., Barrionuevo, F., Dohrmann, U., Günther, T., Schüle, R., Kemler, R., Mallo, M., Kanzler, B., Scherer, G., 2006. Long-range upstream and downstream enhancers control distinct subsets of the complex spatiotemporal Sox9 expression pattern. Dev. Biol. 291, 382-397.

77 Betancur, P., Bronner-Fraser, M., Sauka-Spengler, T., 2010. Genomic code for Sox10 activation reveals a key regulatory enhancer for cranial neural crest. Proc. Natl. Acad. Sci. USA. 107, 3570-3575.

78 Wahlbuhl, M., Reiprich, S., Vogl, M.R., Bösl, M.R., Wegner, M., 2012. Transcription factor Sox10 orchestrates activity of a neural crest-specific enhancer in the vicinity of its gene. Nucleic Acids Res. 40, 88-101.

79 Guenther, M.G., Levine, S.S., Boyer, L.A., Jaenisch, R., Young, R.A., 2007. A chromatin landmark and transcription initiation at most promoters in human cells. Cell 130, 77-88.

80 Kouzarides, T., 2007. Chromatin modifications and their function. Cell 128, 693-705.

81 Nishioka, K., Chuikov, S., Sarma, K., Erdjument-Bromage, H., Allis, C.D., Tempst, P., Reinberg, D., 2002. Set9, a novel histone H3 methyltransferase that facilitates transcription by precluding histone tail modifications required for heterochromatin formation. Genes Dev. 16, 479-489.

82 Schuettengruber, B., Chourrout, D., Vervoort, M., Leblanc, B., Cavalli, G., 2007.

Genome regulation by polycomb and trithorax proteins. Cell 128, 735-745.

83 Lee, J.H., Skalnik, D.G., 2008. Wdr82 is a C-terminal domain-binding protein that recruits the Setd1A Histone H3-Lys4 methyltransferase complex to transcription start sites of transcribed human genes. Mol. Cell Biol. 28, 609-618.

84 Fritsch, L., Robin, P., Mathieu, J.R., Souidi, M., Hinaux, H., Rougeulle, C., Harel-Bellan, A., Ameyar-Zazoua, M., Ait-Si-Ali, S., 2010. A subset of the histone H3 lysine 9 methyltransferases Suv39h1, G9a, GLP, and SETDB1 participate in a multimeric complex. Mol. Cell 37, 46-56.

85 Pan, G., Li, J., Zhou, Y., Zheng, H., Pei, D., 2006. A negative feedback loop of transcription factors that controls stem cell pluripotency and self-renewal. FASEB J. 20, 1730-1732.

86 Guo, Y., Costa, R., Ramsey, H., Starnes, T., Vance, G., Robertson, K., Kelley, M., Reinbold, R., Scholer, H., Hromas, R., 2002. The embryonic stem cell transcription factors Oct-4 and FoxD3 interact to regulate endodermal-specific promoter expression. Proc. Natl. Acad. Sci. USA. 99, 3663-3367.

87 Layman, W.S., Zuo, J., 2015. Epigenetic regulation in the inner ear and its potential roles in development, protection, and regeneration. Front. Cell. Neurosci. 8, 446.

88 Lohmann, F., Loureiro, J., Su, H., Fang, Q., Lei, H., Lewis, T., Yang, Y., Labow, M., Li, E., Chen, T., Kadam, S., 2010. KMT1E mediated H3K9 methylation is required for the

maintenance of embryonic stem cells by repressing trophectoderm differentiation. Stem Cells 28, 201-212.

89 van den Akker, E., Forlani, S., Chawengsaksophak, K., de Graaff, W., Beck, F., Meyer, B.I., Deschamps, J., 2002. Cdx1 and Cdx2 have overlapping functions in anteroposterior patterning and posterior axis elongation. Development 129, 2181-2193.

90 Barnes, R.M., Firulli, B.A., Conway, S.J., Vincentz, J.W., Firulli, A.B., 2010. Analysis of the Hand1 cell lineage reveals novel contributions to cardiovascular, neural crest, extra-embryonic, and lateral mesoderm derivatives. Dev. Dyn. 239, 3086-3097.

91 Fei, Q., Yang, X., Jiang, H., Wang, Q., Yu, Y., Yu, Y., Yi, W., Zhou, S., Chen, T., Lu, C., Atadja, P., Liu, X.S., Li, E., Zhang, Y., Shou, J.. 2015. SETDB1 modulates PRC2 activity at developmental genes independently of H3K9 trimethylation in mouse ES cells. Genome Res. 25, 1325-1335.

Research achievement

Publications

1. Kyohei Fujita, Ryuhei Ogawa, Syunsaku Kawawaki, Kazuo Ito, Roles of chromatin remodelers in maintenance of multipotency of mouse trunk neural crest cells in the formation mechanisms of neural crest-derived stem cells, *Mechanisms of Development*, 133, 126-145, 2014.

2. Kyohei Fujita, Saki Yasui, Takeshi Shinohara, Kazuo Ito, Interaction between NF-κB signaling and Notch signaling in gliogenesis of mouse mesencephalic neural crest cells, *Mechanisms of Development*, 128, 496-509, 2011.

3. Kazuo Ito, Kyohei Fujita, In vivo analysis of mouse mesencephalic neural crest development, *Current Protocols in Neuroscience*, 56, 3.23.1-3.23.8, 2011.

Conference presentation

4. 藤田恭平, 小川竜平, 伊藤一男, マウス神経冠細胞由来幹細胞の形成機構, 1P0972, 第 38 回日本分子生物学会年会, 神戸, 2015 年 12 月

5. 小川竜平, 藤田恭平, 伊藤一男, LIF/BMP2/FGF2 によるマウス後根神経節内神経冠細胞由来多能性幹細胞の分化能維持と増殖, 1P0974, 第 38 回日本分子生物学会年会, 神戸, 2015 年 12 月

6. Ryuhei Ogawa, Kyohei Fujita, Kazuo Ito, Characterization of neural crest-derived stem cells in mouse dorsal root ganglia, Finnish-Japanese joint symposium on Morphogenesis and Signaling, University of Helsinki, Finland, March 3-4, 2015

7. Kyohei Fujita, Ryuhei Ogawa, Syunsaku Kawawaki, Kazuo Ito, Roles of chromatin remodelers in maintenance of multipotency of mouse trunk neural crest cells in the formation mechanisms of neural crest-derived stem cells, Gordon Research Conference on Neural Crest & Cranial Placodes, Stonehill collage, Easton, MA, July 21-26, 2013

8. Kyohei Fujita, Ryuhei Ogawa, Syunsaku Kawawaki, Kazuo Ito, The roles of chromatin remodelers in the maintenance of multipotency of mouse trunk neural crest cells in the relationship with the formation mechanisms of neural crest-derived stem cells, FT4-03, 第 46 回日本発生生物学会年会, 島根, 2013 年 5 月

9. Kyohei Fujita, Ryuhei Ogawa, Syunsaku Kawawaki, Kazuo Ito, The roles of chromatin remodelers in the maintenance of multipotency of mouse trunk neural crest cells in the relationship with the formation mechanisms of neural crest-derived stem cells, P-049, 第 46 回日本発生生物学会年会, 島根, 2013 年 5 月

10. Kyohei Fujita, Kanenobu Ijuin, Kouichi Nakanishi, Keisuke Sugiura, Kazuo Ito, Roles of FGF and Notch signaling in the chondrogenic and gliogenic specification of mouse mesencephalic neural crest cells, P3-025, 第 45 回日本発生生物学会年会, 神戸, 2012 年 5 月

11. Kyohei Fujita, Kazuo Ito, Roles of NF-κB signaling in gliogenesis of mouse

mesencephalic neural crest cells, P-225, 第 43 回日本発生生物学会年会, 京都, 2010 年 6 月